

Equivalence and Unification of the Ballistic and the Kinetic Treatment of Collisional Absorption

Vom Fachbereich Physik
der Technischen Universität Darmstadt

zur Erlangung des Grades
eines Doktors der Naturwissenschaften
(Dr. rer. nat.)

genehmigte Dissertation von
Dipl. -Phys. Ralf Schneider
aus Darmstadt

Referent: Prof. Dr. P. Mulser
Korreferent: Prof. Dr. P. Manakos

Tag der Einreichung: 13.2.2002
Tag der Prüfung: 24.4.2002

Darmstadt 2002
D17

“A reasonable starting point for a discussion of the many-body problem might be the question of how many bodies are required before we have a problem. Prof. G. E. Brown has pointed out that, for those interested in exact solutions, this can be answered by a look at history. In eighteenth-century Newtonian mechanics, the three-body problem was insoluble. With the birth of general relativity around 1910 and quantum electrodynamics in 1930, the two- and one-body problems became insoluble. And within modern quantum field theory, the problem of zero bodies (vacuum) is insoluble. So, if we are out after exact solutions, no bodies at all is already too many.”

[Richard D. Mattuck, *A Guide to Feynman Diagrams in the Many-Body Problem*]

In this work two important models of treating *collisional absorption in a laser driven plasma* are compared, the kinetic and the ballistic model. We will see that there exists a remarkable connection between these basic approaches which could give a hint how to overcome the inherent limitations.

Contents

1	Introduction	3
1.1	The basic mechanism of collisional absorption	4
2	Kinetic Theory	5
2.1	The classical theory	5
2.1.1	The 2-particle distribution function	5
2.1.2	2-particle operators	6
2.1.3	Discussion of the 3-particle part	8
2.1.4	Beyond the weak correlation assumption	9
2.2	The quantum kinetic extension	10
3	Different Models of Collisional Absorption	13
3.1	The kinetic treatment	13
3.1.1	The long-wavelength approximation (LWA) and a remark on the literature	17
3.2	The ballistic treatment	19
3.3	A combined model for collisional absorption	21
3.3.1	The connection between the kinetic and the ballistic treatment . . .	21
3.3.2	The screening length	23
3.3.3	Strong two-body collisions	25
3.3.4	Inclusion of quantum effects	26
3.3.5	The combined absorption result	28
4	Results and Conclusion	30
A	Explicit Expressions for Propagators	35
A.1	Free propagators	35
A.2	Propagators including first order pair interaction	36
B	RPA approximation	38
C	Wigner Representation of the Kinetic Hierarchy	42

Chapter 1

Introduction

For the prediction of collisional absorption - or inverse bremsstrahlung absorption - of electromagnetic radiation in a plasma the dynamics of collisions between particles have to be understood. The process of collisional absorption was of interest during a long time, as it is one of the fundamental heating mechanisms in laser or ion-beam driven plasmas. The progress in laser technology that makes short-pulse laser of high intensity available in experiments brought the interest up again, especially for the absorption of *strong* electromagnetic fields. From the theoretical point of view, the *statistical non equilibrium* properties of the collisional processes in the plasma make studying this field such attractive.

From the early works of Spitzer [1] and Braginskii [2] the collisional absorption rate, as well as the electron-ion collision frequency which relates to one-to-one, for static electric fields is well-known. Studies according to the high-frequency field were also made by Dawson and Oberman [3], by Perl' and Eliashberg [4] and by Silin [5]. The collision frequency in strong fields, which was first discussed by Silin [5], recently has been restudied by Decker *et al.* [6]. Most of these works were limited to classical mechanics and the quantum correction entered only by an ad hoc cut-off - the De Broglie wavelength - which removes the divergency for small impact parameters in the collision integral. Quantum mechanical treatments were first given by Rand [7] and by Schlessinger and Wright [8]. A quantum approach in strong fields was also given by Silin and Uryupin [9]. A quantum mechanical dielectric treatment for arbitrary field strength was recently presented by Kull and Plagne [10] and also by Hazak *et al.* [11] the latter one including ion-ion correlations. Most of these works are based on the Vlasov equation - classical as well as quantum mechanical - including scattering by randomly distributed ions in first order perturbation theory. With the help of the more general Kadanoff-Baym equations including many-particle effects in dense plasmas, see Kremp *et al.* [12], the collision frequency was calculated by Bornath *et al.* [13]. A consistent treatment of dynamic screening at zero temperature was first done by Saemann and Mulser [14][15]. The publications mentioned above present the time-averaged absorption rate. Recently, Mulser *et al.* [16] have discussed the time-dependent absorption rate which was still missing in the literature. The theoretical results have also been confirmed by numerical simulations of the many-body system, see Pfaelzner and Gibbon [18].

In our work we will follow at first the classical and the quantum kinetic approach based

on the first and the second equation of the BBGKY(Bogoliubov, Born, Green, Kirkwood, Yvon)-hierarchy. The hierarchy will be closed using the *random phase approximation* (RPA). Because the dielectric function of the plasma occurs in the RPA, this treatment is also called the *dielectric model*. We then will extend this approximation with the help of the *ballistic model* [16] which includes strong two-body collisions.

It is our main concern to achieve a single expression for the time-averaged collisional absorption rate valid in a large parameter region which no longer includes integrals or sums over an infinite range. Such an expression is still missing in the literature. Mostly the publications end up with expressions which are still very complicated. Only asymptotic approximations of those are presented in form of standard Coulomb logarithms.

1.1 The basic mechanism of collisional absorption

Imagine a homogeneous infinite plasma. It is considered to be quasi neutral, that is, if the ion density is n_i we expect the electron density to be $n_e = Zn_i$, where Z is the charge state of the ions. So, the overall electric and magnetic fields are zero. The plasma is disturbed by a time-dependent outer field, for example the oscillating electric field of a laser. The first process we observe is the oscillation of the electrons. In general, energy conversion between the electromagnetic field and matter is governed by Poynting's theorem. The coupling between the field and the matter is expressed in the source term $\vec{j}\vec{E}$. In a time periodic electric field the cycle average of this term gives us the energy conversion rate, i. e. the absorption. As long as we assume total homogeneity the current density $\vec{j}(t)$ follows the electric field $\vec{E}(t)$ and the time average of the scalar product is zero. What we need is a *phase shift* between the current density and the applied field. This phase shift is induced by inhomogeneities in the density. One distinguishes between microscopic inhomogeneities, fluctuations, and macroscopic ones, density gradients. The second kind involves a large amount of particles and exists on the hydrodynamic or mean field scale leading to the so called *collective* absorption; whereas the first one has its origin in the graininess of matter and brings up *collisional* absorption. Our calculation model has to resolve the scale of graininess, that is, the particle-particle scattering has to be described. These scattering events give rise to the phase shift between the current density and the electric field.

Chapter 2

Kinetic Theory

In this chapter we will introduce the basic description of the plasma processes we are interested in. It is the non equilibrium kinetic theory based on the BBGKY-hierarchy. As this theory is well known only the specific parts which are important for our discussion will be mentioned. We will start with the classical theory and later we shall switch to the Wigner description of the quantum kinetic treatment. We shall take advantage of a symbolic, diagrammatic formalism to conserve the form of the equations in the classical as well as in the quantum mechanical case. The basic concepts can be found in [26][24][25][23].

2.1 The classical theory

2.1.1 The 2-particle distribution function

In the conventional way we write down the Liouville operator depending on the two-particle interaction potential Φ_{jk} and the potential of an external field Φ^{ex} :

$$\mathcal{L}_{1\dots s} = \sum_{j=1}^s -\frac{i}{m} \vec{p}_j \frac{\partial}{\partial \vec{r}_j} + i \frac{\partial \Phi^{\text{ex}}}{\partial \vec{r}_j} \frac{\partial}{\partial \vec{p}_j} , \quad \mathcal{V}_{jk} = i \frac{\partial \Phi_{jk}}{\partial \vec{r}_j} \left(\frac{\partial}{\partial \vec{p}_j} - \frac{\partial}{\partial \vec{p}_k} \right) , \quad \mathcal{L}'_{12} = \mathcal{L}_{12} + \mathcal{V}_{12} . \quad (2.1)$$

The second equation of the classical BBGKY-hierarchy for the 2-particle distribution function is

$$\begin{aligned} \left(\frac{\partial}{\partial t} + i \mathcal{L}'_{12} \right) f_2(1, 2, t) &= - \int d3 \, (i \mathcal{V}_{13} + i \mathcal{V}_{23}) f_3(1, 2, 3, t) \\ &= I(1, 2, [3], t) . \end{aligned} \quad (2.2)$$

The momentum and position arguments of the distribution functions as well as the phase space integrals, including summation over particle species, are shortened by notating the particle number only.

In order to get a diagrammatic formalism, the following abbreviations are introduced:

Propagation of particles j and k for a time $+\tau$: $\uparrow_{jk}^\tau = e^{-i \int_0^\tau \mathcal{L}_{jk}}$
 Propagation of particles j and k for a time $-\tau$: $\downarrow_{jk}^\tau = e^{+i \int_0^\tau \mathcal{L}_{jk}}$
 Interaction of the particles j and k : $\sim\sim\sim = -i\mathcal{V}_{jk}$

Propagation and interaction of two particles:

$$\left| \begin{array}{c} \sim\sim\sim \\ \sim\sim\sim \end{array} \right| = \int_0^{\tau'} \downarrow_{12}^\tau \sim\sim\sim \uparrow_{12}^\tau$$

Propagation and interaction of two particles in the mean field of a third one:

$$\left| \begin{array}{c} \sim\sim\sim \\ \sim\sim\sim \end{array} \right| = \int_0^{\tau''} \int d2 \downarrow_{23}^{\tau'} \sim\sim\sim \uparrow_{23}^{\tau'} \int_0^{\tau'} \downarrow_{12}^\tau \sim\sim\sim \uparrow_{12}^\tau$$

The differential equation for the 2-particle distribution function Eq. (2.2) can be transformed into an integral equation:

$$f_2(1, 2, t) = e^{-i \int_0^t \mathcal{L}'_{12} d\tau'} f_2^0 + \int_0^t e^{-i \int_\tau^t \mathcal{L}'_{12} d\tau'} I(1, 2, [3], \tau) d\tau . \quad (2.3)$$

Using the defined symbols we get

$$\begin{aligned} f_2(1, 2, t) = & \uparrow_{12}^t f_2^0 + \uparrow_{12}^t \int_0^t \downarrow_{12}^\tau \sim\sim\sim f_2(1, 2, \tau) d\tau \\ & + \uparrow_{12}^t \int_0^t \downarrow_{12}^\tau \int d3 \left(\overset{1}{\sim\sim\sim}^3 + \overset{2}{\sim\sim\sim}^3 \right) f_3(1, 2, 3, \tau) d\tau \end{aligned} \quad (2.4)$$

This integral equation has to be solved by iteration. To do so we have to close the equation by finding a consistent approximation for the three-particle part. Before discussing this closure of the hierarchy we pay attention to the 2-particle operators.

2.1.2 2-particle operators

The propagator $e^{-i \int_\tau^t \mathcal{L}'_{12}}$ includes the pair interaction as well as the external field. To examine in which way they act onto the 2-particle functions, we neglect the 3-particle part in Eq. (2.2),(2.3) and move the pair interaction to the right side:

$$\left(\frac{\partial}{\partial t} + i\mathcal{L}_{12}^0 \right) f_2(1, 2, t) = -i\mathcal{V}_{12} f_2(1, 2, t) \quad (2.5)$$

$$f_2(1, 2, t) = e^{-it\mathcal{L}_{12}^0} f_2^0 - \int_0^t e^{-i(t-\tau)\mathcal{L}_{12}^0} i\mathcal{V}_{12} f_2(1, 2, \tau) d\tau . \quad (2.6)$$

If the external field is absent, $\mathcal{L}_{12} = \mathcal{L}_{12}^0$, the propagator \uparrow_{12}^τ is a pure shift operator,

$$\uparrow_{12}^\tau f_2(\vec{r}_1, \vec{p}_1, \vec{r}_2, \vec{p}_2) = f_2\left(\vec{r}_1 - \tau \frac{\vec{p}_1}{m_1}, \vec{p}_1, \vec{r}_2 - \tau \frac{\vec{p}_2}{m_2}, \vec{p}_2\right) ,$$

describing the free propagations of the particles. It obviously separates into several one-particle parts, $\uparrow_{12}^\tau = \uparrow_1^\tau \uparrow_2^\tau$.

Writing Eq. (2.6) using the defined symbols,

$$f_2(1, 2, t) = \uparrow_{12}^t f_2^0 + \uparrow_{12}^t \int_0^t \downarrow_{12}^\tau \sim f_2(1, 2, \tau) d\tau, \quad (2.7)$$

and solving it by iteration, we find the known *ladder*-diagrams:

$$f_2(1, 2, t) = \left| \begin{array}{c} | \\ | \\ | \end{array} \right| + \left| \begin{array}{c} | \\ \sim \\ | \end{array} \right| + \left| \begin{array}{c} | \\ \sim \\ \sim \\ | \end{array} \right| + \left| \begin{array}{c} | \\ \sim \\ \sim \\ \sim \\ | \end{array} \right| + \dots \quad (2.8)$$

$$\begin{aligned} &= \uparrow_{12}^t f_2^0 \\ &+ \uparrow_{12}^t \int_0^t \downarrow_{12}^\tau \sim \uparrow_{12}^\tau f_2^0 \\ &+ \uparrow_{12}^t \int_0^t \downarrow_{12}^\tau \sim \uparrow_{12}^\tau \int_0^\tau \downarrow_{12}^{\tau'} \sim \uparrow_{12}^{\tau'} f_2^0 \\ &+ \uparrow_{12}^t \int_0^t \downarrow_{12}^\tau \sim \uparrow_{12}^\tau \int_0^\tau \downarrow_{12}^{\tau'} \sim \uparrow_{12}^{\tau'} \int_0^{\tau'} \downarrow_{12}^{\tau''} \sim \uparrow_{12}^{\tau''} f_2^0 \\ &+ \dots \\ &= e^{-it\mathcal{L}_{12}^0} e^{-i\int_0^t e^{i\tau\mathcal{L}_{12}^0} \mathcal{V}_{12} e^{-i\tau\mathcal{L}_{12}^0} f_2^0 d\tau} \\ &= e^{-it\mathcal{V}_{12}} e^{-i\int_0^t e^{i\tau\mathcal{V}_{12}} \mathcal{L}_{12}^0 e^{-i\tau\mathcal{V}_{12}} f_2^0 d\tau}. \end{aligned} \quad (2.9)$$

$$(2.10)$$

The exponential form of this operator is built up by partial integration of the time integrals.

In detail, setting $F(\tau') = \int_0^{\tau'} \downarrow_{12}^{\tau''} \sim \uparrow_{12}^{\tau''}$:

$$\downarrow_{12}^{\tau'} \sim \uparrow_{12}^{\tau'} \int_0^{\tau'} \downarrow_{12}^{\tau''} \sim \uparrow_{12}^{\tau''} = \frac{\partial F(\tau')}{\partial \tau'} F(\tau') = \frac{1}{2} \frac{\partial F^2(\tau')}{\partial \tau'}.$$

The second form of the ladder-propagator, Eq. (2.10), is calculated by replacing the free propagator \mathcal{L}_{12}^0 by the interaction one in Eq. (2.5) and solving the appropriate integral equation. The explicit expression of this propagator is quite complicated. It is no longer a pure shift operator as it contains the particle interaction. Nevertheless, as the 3-particle term is not included, this propagator describes the two-body problem of which the implicit solution is well known as long as no external field is switched on.

Using the above iteration scheme we could determine the free propagator including an external field depending on the time, but not on the position. The same procedure as before

in which the pair interaction is replaced by the Liouville operator of the electric field of the laser in dipole approximation,

$$\mathcal{V}_{12} = \mathcal{L}^{\text{ex}} = \sum_{j=1}^2 i \frac{\partial \Phi^{\text{ex}}}{\partial \vec{r}_j} \frac{\partial}{\partial \vec{p}_j} = i \vec{E}(t) \left(q_1 \frac{\partial}{\partial \vec{p}_1} + q_2 \frac{\partial}{\partial \vec{p}_2} \right) \quad [q_1, q_2 \text{ charges of the particles}],$$

leads us to:

$$\begin{aligned} \uparrow_{12}^t &= e^{-i \int_0^t \mathcal{L}_{12}} = e^{-i \int_0^t \mathcal{L}_{12}^0 + \mathcal{L}_{12}^{\text{ex}}} \\ &= e^{-i \int_0^t \mathcal{L}_{12}^{\text{ex}}} e^{-i \int_0^t e^{i \int_0^\tau \mathcal{L}_{12}^{\text{ex}}} \mathcal{L}_{12}^0 e^{-i \int_0^\tau \mathcal{L}_{12}^{\text{ex}}} d\tau} \end{aligned}$$

This propagator separates into 1-particle propagators, $\uparrow_{12}^t = \uparrow_1^t \uparrow_2^t$, and acts as a shift operator in momentum and position, solving Newton's equation. The calculation is done in detail in Appendix A and results in Eq. (A.1):

$$\uparrow_1^t = e^{-q_1 \int_0^t \vec{E} \cdot \frac{\partial}{\partial \vec{p}_1}} e^{-\frac{1}{m_1} (t \vec{p}_1 + q_1 \int_0^t \int_0^\tau \vec{E}) \cdot \frac{\partial}{\partial \vec{r}_1}}. \quad (2.11)$$

2.1.3 Discussion of the 3-particle part

To solve the integral equation for the 2-particle distribution function, Eq. (2.4), we have to find a closure due to the 3-particle source term. We extract the 3-particle correlation part

$$\begin{aligned} f_2(1, 2) &= f(1)f(2) + g_2(1, 2) \\ f_3(1, 2, 3) &= f(1)f(2)f(3) + f(1)g_2(2, 3) + f(2)g_2(1, 3) + f(3)g_2(1, 2) + g_3(1, 2, 3). \end{aligned}$$

Assuming that all particles are uncorrelated at the beginning, $g_2^0 = g_3^0 = \dots = 0$ when supposing an ideal, fully ionized plasma in equilibrium, all correlations have to be built up dynamically through the processes we incorporate. Correlations due to the particle exchange symmetry, Fermi and Bose statistics, can be included by (anti)symmetrization of the pair operators [23]. This case will not be considered in this work as we assume that we are far away from the degenerated case.

If the average kinetic energy of the particles is much larger than the average potential energy, the interaction between the particles can be handled by the first order Born approximation. All graphs in which two particles are connected with *more than one* interaction line are *neglected*. The 3-particle correlation consists of all graphs in which three particles are irreducibly connected. To be consistent we have to neglect the contribution of g_3 in $I(1, 2, [3], t)$ because these parts of $I(1, 2, [3], t)$ would contain second order interaction terms. For example, the contribution of the most simple diagram of g_3 is:

$$\int d3 (i\mathcal{V}_{13} + i\mathcal{V}_{23}) \left| \begin{array}{c} \text{---} \text{---} \text{---} \\ \text{---} \text{---} \end{array} \right| = \left| \begin{array}{c} \text{---} \text{---} \text{---} \\ \text{---} \text{---} \end{array} \right| + \left| \begin{array}{c} \text{---} \text{---} \text{---} \\ \text{---} \text{---} \end{array} \right| \approx 0.$$

Based on this approximation the integral equation (2.4) can be solved. It results in the sum of all diagrams which contain only one interaction line between two 1-particle propagators, the well known *Random Phase Approximation* (RPA) [26][24][25][23]:

$$f_2(1, 2, t) = \left| \begin{array}{c} \text{---} \\ \text{---} \end{array} \right| + \left| \begin{array}{c} \text{---} \text{---} \\ \text{---} \end{array} \right| + \left| \begin{array}{c} \text{---} \text{---} \text{---} \\ \text{---} \end{array} \right| + \left| \begin{array}{c} \text{---} \text{---} \text{---} \\ \text{---} \text{---} \end{array} \right| + \dots \quad (2.12)$$

2.2 The quantum kinetic extension

At first inspection, the quantum kinetic approach seems to be very different compared to the classical one. But if we choose the Wigner representation the form of the equations will remain the same, only the interaction operators will be obviously different. The transition from the quantum mechanical BBGKY-hierarchy in coordinate representation to the Wigner representation is shown in Appendix C.

We write the second equation of the BBGKY-hierarchy in Wigner representation (spin variables are suppressed):

$$\left(\frac{\partial}{\partial t} + \frac{p_1}{m_1} \frac{\partial}{\partial R_1} + \frac{p_2}{m_1} \frac{\partial}{\partial R_2} \right) f_2(R_1, p_1, R_2, p_2, t) + \frac{i}{\hbar} (F_{12} + F_1^{ex} + F_2^{ex}) = \frac{i}{\hbar} (F_1^3 + F_2^3) \quad (2.14)$$

with $[R_{12} = R_1 - R_2, r_{12} = r_1 - r_2]$

$$\begin{aligned} F_{12} &= \int \frac{dr_{12}}{(2\pi\hbar)^3} d\eta_1 e^{-\frac{i}{\hbar}(p_1-\eta_1)r_{12}} \left(\Phi(R_{12} + \frac{r_{12}}{2}) - \Phi(R_{12} - \frac{r_{12}}{2}) \right) \\ &\times f_2(R_1, \eta_1, R_2, p_2 + p_1 - \eta_1, t) , \\ F_i^{ex} &= \int \frac{dr_i}{(2\pi\hbar)^3} d\eta_i e^{-\frac{i}{\hbar}(p_i-\eta_i)r_i} \left(\Phi^{ex}(R_i + \frac{r_i}{2}, t) - \Phi^{ex}(R_i - \frac{r_i}{2}, t) \right) \\ &\times f_2(R_1, \eta_1, R_i, p_i, t) , \\ F_i^3 &= \int \frac{dr_i}{(2\pi\hbar)^3} d\eta_i dR_3 dp_3 e^{-\frac{i}{\hbar}(p_i-\eta_i)r_i} \left(\Phi(R_{i3} + \frac{r_i}{2}) - \Phi(R_{i3} - \frac{r_i}{2}) \right) \\ &\times f_3(R_1, \eta_1, R_i, p_i, R_3, p_3, t) . \end{aligned}$$

The binary interaction operator is

$$\begin{aligned} \sim\sim &= \sim\sim_+ + \sim\sim_- = \sum_{\pm} \sim\sim_{\pm} \\ \sim\sim_{\pm} &= \pm \frac{1}{i\hbar} \int \frac{dr_{12} d\eta_1}{(2\pi\hbar)^3} e^{-\frac{i}{\hbar}(p_1-\eta_1)r_{12}} \Phi(R_{12} \pm r_{12}/2) \\ &= \pm \frac{1}{i\hbar} \int dk \Phi_k \int \frac{dr_{12} d\eta_1}{(2\pi\hbar)^3} e^{-\frac{i}{\hbar}(p_1-\eta_1)r_{12}} e^{ik(R_{12} \pm r_{12}/2)} \\ &= \pm \frac{1}{i\hbar} \int dk \Phi_k \int \frac{dr_{12} d\eta_1}{(2\pi\hbar)^3} e^{-\frac{i}{\hbar}(p_1-\eta_1 \mp \hbar k/2)r_{12}} e^{ikR_{12}} \\ &= \pm \frac{1}{i\hbar} \int dk \Phi_k \int d\eta_1 \delta(\eta_1 - p_1 \pm \hbar k/2) e^{ikR_{12}} \end{aligned}$$

The last step in the above calculation can be done, due to the operator $\sim\sim_{\pm}$ acting onto functions with a dependency of $f_2(R_1, \eta_1, R_2, p_2 + p_1 - \eta_1)$. These are independent of r_{12} . So, the interaction potential Φ_{12} in Eq. (2.14) can be written as

$$\begin{aligned}
\sim f_2 &= \sum_{\pm} \sim_{\pm} f_2 \\
&= \sum_{\pm} \pm \frac{1}{i\hbar} \int dk \Phi_k \int d\eta_1 \delta(\eta_1 - p_1 \pm \hbar k/2) e^{ikR_{12}} f_2(R_1, \eta_1, R_2, p_2 + p_1 - \eta_1) \\
&= \frac{1}{i\hbar} \int dk \Phi_k e^{ikR_{12}} f_k^-(R_1, p_1, R_2, p_2) \\
&= \frac{1}{i\hbar} \int dk \Phi_k e^{ikR_{12}} \left(e^{\frac{\hbar k}{2}(\frac{\partial}{\partial p_2} - \frac{\partial}{\partial p_1})} - e^{-\frac{\hbar k}{2}(\frac{\partial}{\partial p_2} - \frac{\partial}{\partial p_1})} \right) f_2(R_1, p_1, R_2, p_2) \\
&= \frac{2i}{\hbar} \int dk \Phi_k e^{ikR_{12}} \sinh \left[\frac{\hbar k}{2} \left(\frac{\partial}{\partial p_1} - \frac{\partial}{\partial p_2} \right) \right] f_2(R_1, p_1, R_2, p_2)
\end{aligned} \tag{2.15}$$

with

$$f_k^-(R_1, p_1, R_2, p_2) = f_2(R_1, p_1 - \hbar k/2, R_2, p_2 + \hbar k/2) - f_2(R_1, p_1 + \hbar k/2, R_2, p_2 - \hbar k/2) .$$

The transition to the classical expression is easily done by an expansion of the sinh-term up to first order of \hbar .

Also, the three-particle terms F_i^3 and the external Potentials F_i^{ex} in Eq. (2.14) can be written as

$$\begin{aligned}
F_i^3 &= \frac{2i}{\hbar} \int dR_3 dp_3 \int dk \Phi_k e^{ikR_{i3}} \sinh \left[\frac{\hbar k}{2} \left(\frac{\partial}{\partial p_i} - \frac{\partial}{\partial p_3} \right) \right] f_3(R_1, p_1, R_i, p_i, R_3, p_3) \\
F_i^{ex} &= \frac{2i}{\hbar} \int dk \Phi_k^{ex} e^{ikR_i} \sinh \left[\frac{\hbar k}{2} \frac{\partial}{\partial p_i} \right] f_2(R_1, p_1, R_i, p_i) .
\end{aligned}$$

In case the external force depends on the time only, as e.g. the electric field of the laser in dipole approximation, the above expression for F_i^{ex} reduces to the classical one:

$$F_i^{ex} = q_i \vec{E}(t) \frac{\partial}{\partial \vec{p}_i} f_2(R_1, p_1, R_i, p_i) .$$

The quantum kinetic equation for the 2-particle Wigner function now reaches the same structure as the classical one, Eq. (2.4):

$$\begin{aligned}
f_2(1, 2, t) = & \uparrow_{12}^t f_2^0 + \uparrow_{12}^t \int_0^t \downarrow_{12}^\tau \sim f_2(1, 2, \tau) d\tau \\
& + \uparrow_{12}^t \int_0^t \downarrow_{12}^\tau \int d3 \left(\overset{1}{\sim} \overset{3}{\sim} + \overset{2}{\sim} \overset{3}{\sim} \right) f_3(1, 2, 3, \tau) d\tau
\end{aligned} \tag{2.16}$$

with

$$\begin{aligned}
\overset{i}{\sim} \overset{j}{\sim} &= \frac{2i}{\hbar} \int dk \Phi_k e^{ikR_{12}} \sinh \left[\frac{\hbar k}{2} \left(\frac{\partial}{\partial p_1} - \frac{\partial}{\partial p_2} \right) \right] \\
(\text{dipole approx., Eq. (2.11)}) \quad \uparrow_1^\tau &= e^{-q_1 \int_0^\tau \vec{E} \frac{\partial}{\partial \vec{p}_1}} e^{-\frac{1}{m_1}(\tau \vec{p}_1 + q_1 \int_0^\tau \int_0^{\tau'} \vec{E}) \frac{\partial}{\partial \vec{r}_1}} .
\end{aligned}$$

This is straightforward for all the levels of the BBGKY-hierarchy. The discussions about the closure of the hierarchy in the preceding sections remain valid.

Chapter 3

Different Models of Collisional Absorption

In the following chapter two models for calculating energy absorption in a laser plasma will be presented. Each model is valid under the following assumptions:

- The electric field of the laser is treated in dipole approximation. The magnetic field is neglected.
- The electron and ion motion is nonrelativistic.
- We will use the test particle assumption: The ion distribution is described as one delta-like ion plus a homogenous background. This approximation is based on the assumption that only weak many-body collisions occur. These are described in first Born approximation which allows the independent summation over the collision events. (See the discussion in Sec. 2.1.4.)
- The plasma is not degenerate, $T_e > T_{\text{Fermi}}$.

3.1 The kinetic treatment

We calculate the energy absorption by using the RPA results from appendix B. We work on the quantum kinetic expressions. The classical result is easily obtained by the limit $\hbar \rightarrow 0$. The absorbed energy density of the electrons at a time t in general is given by the scalar product of the current and the electric field, $\dot{\mathcal{E}}(\vec{r}_e, t) = \vec{j}_e(\vec{r}_e, t) \vec{E}(\vec{r}_e, t)$. We split the electric field into the oscillating laser part $\vec{E}_L(t)$, the Coulomb field of the ion $\vec{E}_c(\vec{r}_e)$ and the induced field generated by the disturbed electron density $\vec{E}_I(\vec{r}_e, t)$. In addition, the electron current is separated into a free oscillating part $\vec{j}_{\text{os}}(t)$ and an induced one $\vec{j}_I(\vec{r}_e, t)$. We now refer to the reference system of the free oscillating electrons. In the expression for the absorbed energy density the oscillating parts of the electric field and the current vanish. The time dependence of the laser field translates the time dependence of the Coulomb field of the ion because in the comoving frame the ion oscillates. We get

$$\dot{\mathcal{E}}(\vec{r}_e, t) = \vec{j}_I(\vec{r}_e, t) \vec{E}_c(\vec{r}_e, t) + \vec{j}_I(\vec{r}_e, t) E_I(\vec{r}_e, t) = \dot{\mathcal{E}}^{(1)} + \dot{\mathcal{E}}^{(2)} .$$

The second term is of second order in the induced electron density, so we neglect it. Due to the system change the zeroth order $\vec{j}_{\text{os}}(t)\vec{E}_{\text{L}}(t)$ does not appear which has no further meaning as the cycle average of this term is zero.

The system change applies onto the electron distribution function f_e^{qu} , Appendix B [Eq. (B.5)], due to

$$\vec{p}_e \rightarrow \vec{p}_e - e \int_0^t \vec{E}_{\text{L}} \quad , \quad \vec{r}_e \rightarrow \vec{r}_e - \frac{e}{m_e} \int_0^t \int_0^\tau \vec{E}_{\text{L}} \quad .$$

Considering the action of the shift operator \uparrow_e^t , Eq. (2.11), the electron distribution function in the oscillating system assumes the form

$$\begin{aligned} f_e^{\text{qu}}(\vec{r}_e, \vec{p}_e, t) &= f_e^0(p_e) - \frac{2n_e^0}{\hbar(2\pi)^{3/2}v_e^3m_e^3} \int_0^t \int \frac{d^3k}{(2\pi)^3} \Phi_{\text{eff}}^{\text{qu}}(\vec{r}_0, \vec{k}, \tau) \\ &\quad \times e^{-i\vec{k}(\vec{r}_e - \frac{t-\tau}{m_e}\vec{p}_e)} e^{-\frac{p_e^2}{2v_e^2m_e^2} - \frac{k^2}{2k_{\text{B}}^2}} \sinh\left(\frac{\vec{k}\vec{p}_e}{k_{\text{B}}v_em_e}\right) \quad . \end{aligned}$$

Before calculating the current we make some further simplifications. i) We shift the zero point of the time to minus infinity and assume that the laser is smoothly switched on: $\int_0^t \rightarrow \int_0^\infty$, $\tau \rightarrow t - \tau$. Thereby we lose the transient time behavior at the beginning which is of no high interest. ii) The ion temperature is set to zero. iii) The ion mass is set to infinity. iv) The ion position in the lab frame \vec{r}_0 is set to zero.

Using a Fourier expansion for the phase factors containing the electric field $\vec{E}_{\text{L}}(\tau) = \vec{E}_0 \cos \omega_0 \tau$

$$\begin{aligned} e^{-i\vec{k}\vec{\eta}_{ei}(\tau)} &\stackrel{m_i \rightarrow \infty}{=} e^{-i\vec{k}\vec{\eta}_e(\tau)} = e^{-i\vec{k}\frac{e}{m_e} \int_0^\tau \int_0^{\tau'} \vec{E}_{\text{L}}(\tau'') = e^{i\vec{k}\frac{e\vec{E}_0}{m_e\omega_0^2} \cos \omega_0 \tau} = e^{i\vec{k}\vec{r}_{\text{os}} \cos \omega_0 \tau} \\ &= \sum_{l=-\infty}^{l=+\infty} i^l e^{il\omega_0 \tau} J_l(\vec{k}\vec{r}_{\text{os}}) \quad , \end{aligned}$$

the effective potential, Eq. (B.9), expands to

$$\Phi_{\text{eff}}(\vec{k}, \tau) = \int_{c-i\infty}^{c+i\infty} \frac{ds}{2\pi} e^{s\tau} \frac{\Phi_{ei}(k)}{\epsilon(k, s)} \sum_{l=-\infty}^{l=+\infty} i^l \frac{J_l(\vec{k}\vec{r}_{\text{os}})}{s - il\omega_0} \quad .$$

We consider a stable plasma, that is, the zeros of $\epsilon(k, s)$ are damped. So the poles at $s = il\omega_0$ determine the time behavior of $\Phi_{\text{eff}}(\vec{k}, \tau)$

$$\Phi_{\text{eff}}(\vec{k}, \tau) = \Phi_{ei}(k) \sum_{l=-\infty}^{l=+\infty} i^l e^{il\omega_0 \tau} \frac{J_l(\vec{k}\vec{r}_{\text{os}})}{\epsilon(k, il\omega_0)} \quad . \quad (3.1)$$

Calculating the induced current of the electrons $\vec{j}_{\text{I}}^{\text{qu}} = -\frac{e}{m_e} \int d^3p_e \vec{p}_e f_e^{\text{qu}}$ leads to

$$\begin{aligned}
\vec{j}_1^{\text{qu}}(\vec{r}_e, t) &= \frac{en_e^0}{m_e} \sum_{l=-\infty}^{l=+\infty} i^l e^{il\omega_0 t} \int \frac{d^3k}{(2\pi)^3} e^{-i\vec{k}\vec{r}_e} \frac{\vec{k}}{k} \Phi_{ei}(k) \frac{J_l(\vec{k}\vec{r}_{\text{os}})}{\epsilon(k, il\omega_0)} \\
&\quad \times \int_0^\infty d\tau e^{-il\omega_0 \tau} e^{-\frac{1}{2}k^2 v_e^2 \tau^2} \left[\cos\left(\frac{k^2 v_e \tau}{k_B}\right) - k_B v_e \tau \sin\left(\frac{k^2 v_e \tau}{k_B}\right) \right] \\
&= \frac{en_e^0}{m_e v_e} \sqrt{\frac{\pi}{2}} \sum_{l=-\infty}^{l=+\infty} i^l e^{il\omega_0 t} \int \frac{d^3k}{(2\pi)^3} e^{-i\vec{k}\vec{r}_e} \frac{\vec{k}}{k} \Phi_{ei}(k) \frac{J_l(\vec{k}\vec{r}_{\text{os}})}{\epsilon(k, il\omega_0)} \mathcal{G}^{\text{qu}}(k, l\omega_0)
\end{aligned}$$

with

$$\begin{aligned}
\mathcal{G}^{\text{qu}}(k, \omega) &= \frac{k_B}{2v_e} \frac{\omega}{k^2} e^{-\frac{1}{2}\left(\frac{\omega}{kv_e} - \frac{k}{k_B}\right)^2} \\
&\quad \times \left[\text{erfc}\left(\frac{i\omega}{\sqrt{2}kv_e} - \frac{ik}{\sqrt{2}k_B}\right) - e^{-\frac{2\omega}{k_B v_e}} \text{erfc}\left(\frac{i\omega}{\sqrt{2}kv_e} + \frac{ik}{\sqrt{2}k_B}\right) \right]. \quad (3.2)
\end{aligned}$$

In the classical limit, $\hbar \rightarrow 0$ or $k_B \rightarrow \infty$, the function $\mathcal{G}^{\text{qu}}(k, \omega)$ strongly simplifies to

$$\mathcal{G}(k, \omega) = \left(\frac{\omega}{kv_e}\right)^2 e^{-\frac{1}{2}\left(\frac{\omega}{kv_e}\right)^2} \text{erfc}\left(\frac{i\omega}{\sqrt{2}kv_e}\right). \quad (3.3)$$

The total energy absorption rate per ion in RPA approximation can now be determined by

$$\begin{aligned}
\dot{E}_{\text{RPA}}^{\text{qu}}(t) &= \int d^3r_e \vec{j}_1^{\text{qu}}(\vec{r}_e, t) \vec{E}_c(\vec{r}_e, t) \\
&= \frac{Ze}{4\pi\epsilon_0} \int d^3r_e \vec{j}_1^{\text{qu}}(\vec{r}_e, t) \frac{\vec{r}_e - \vec{r}_i(t)}{|\vec{r}_e - \vec{r}_i(t)|^3} \\
&= -\frac{Ze^2 n_e^0}{\epsilon_0 m_e v_e} \sqrt{\frac{\pi}{2}} \sum_{l=-\infty}^{l=+\infty} i^l e^{il\omega_0 t} \int \frac{d^3k}{(2\pi)^3} e^{-i\vec{k}\vec{r}_i(t)} \frac{\Phi_{ei}(k)}{k} \frac{J_l(\vec{k}\vec{r}_{\text{os}})}{\epsilon(k, il\omega_0)} \mathcal{G}^{\text{qu}}(k, l\omega_0)
\end{aligned}$$

Due to the oscillating reference system the position of the ion is $\vec{r}_i(t) = \frac{e\vec{E}_0}{m_e \omega_0^2} \cos \omega_0 t$.

We fix the electric field of the laser in z-direction, $\vec{E}_0 = E_0 \vec{e}_z$. The above expression depends now on k_z and k only. In spherical coordinates we have $k_z = k \cos \theta$, $d^3k = k^2 dk \sin \theta d\theta d\phi$ and the k integration simplifies to

$$\begin{aligned}
\dot{E}_{\text{RPA}}^{\text{qu}}(t) &= -\frac{Ze^2 n_e^0}{\epsilon_0 m_e v_e} \sqrt{\frac{\pi}{2}} \sum_{l=-\infty}^{l=+\infty} i^l e^{il\omega_0 t} \int_0^\infty \frac{dk}{(2\pi)^2} \frac{k \Phi_{ei}(k)}{\epsilon(k, il\omega_0)} \mathcal{G}^{\text{qu}}(k, l\omega_0) \\
&\quad \times \int_{-1}^1 dx e^{-ikr_{\text{os}} x \cos \omega_0 t} J_l(kr_{\text{os}} x) \\
&= -\frac{Ze^2 n_e^0}{\epsilon_0 m_e v_e} \sqrt{\frac{\pi}{2}} \sum_{l,m=-\infty}^{\infty} (-1)^{m_i(l+m)} e^{i(l+m)\omega_0 t} \int_0^\infty \frac{dk}{(2\pi)^2} \frac{k \Phi_{ei}(k)}{\epsilon(k, il\omega_0)} \mathcal{G}^{\text{qu}}(k, l\omega_0)
\end{aligned}$$

$$\times \int_{-1}^1 dx J_l(kr_{\text{os}}x) J_m(kr_{\text{os}}x) . \quad (3.4)$$

The above expression determines the *time-dependent absorption rate*. Further we are interested in the cycle-averaged rate which usually is analyzed in the literature. Averaging over one laser cycle we get

$$\begin{aligned} \overline{\dot{E}_{\text{RPA}}^{\text{qu}}} &= -\frac{Ze^2n_e^0}{\epsilon_0m_ev_e}\sqrt{\frac{\pi}{2}}\sum_{l,m=-\infty}^{\infty}(-1)^{m_i(l+m)}\delta_{m,-l}\int_0^{\infty}\frac{dk}{(2\pi)^2}\frac{k\Phi_{ei}(k)}{\epsilon(k,i\omega_0)}\mathcal{G}^{\text{qu}}(k,l\omega_0) \\ &\times \int_{-1}^1 dx J_l(kr_{\text{os}}x) J_m(kr_{\text{os}}x) \\ &= -\frac{2Ze^2n_e^0}{\epsilon_0m_ev_e}\sqrt{\frac{\pi}{2}}\sum_{l=-\infty}^{\infty}\int_0^{\infty}\frac{dk}{(2\pi)^2}\frac{k\Phi_{ei}(k)}{\epsilon(k,i\omega_0)}\mathcal{G}^{\text{qu}}(k,l\omega_0) \\ &\times \int_0^1 dx J_l^2(kr_{\text{os}}x) . \end{aligned}$$

According to the complex conjugation (*) the dielectric function $\epsilon(k,i\omega)$, Eq. (B.6), as well as the function $\mathcal{G}(k,\omega)$, Eq. (3.2, 3.3), exhibit the symmetry property

$$\epsilon(k,-i\omega) = \epsilon^*(k,i\omega) , \quad \mathcal{G}(k,-\omega) = \mathcal{G}^*(k,\omega)$$

for real frequencies and wavenumbers. Furthermore we see that $\mathcal{G}(k,\omega=0)=0$, that is, the static part [$l=0$] does not contribute to the absorption. The expression for the absorption simplifies to

$$\begin{aligned} \overline{\dot{E}_{\text{RPA}}^{\text{qu}}} &= -\frac{4Ze^2n_e^0}{\epsilon_0m_ev_e}\sqrt{\frac{\pi}{2}}\sum_{l=1}^{\infty}\int_0^{\infty}\frac{dk}{(2\pi)^2}\Phi_{ei}(k)\Re\left\{\frac{\mathcal{G}^{\text{qu}}(k,l\omega_0)}{\epsilon(k,i\omega_0)}\right\} \\ &\times \int_0^1 dx J_l^2(kr_{\text{os}}x) . \end{aligned}$$

For the real and imaginary parts (\Re, \Im) of the functions \mathcal{G} and ϵ we find (k, ω real) in the quantum mechanical as well as in the classical case

$$\Re\{\mathcal{G}^{\text{qu}}(k,\omega)\} = \frac{k_{\text{B}}}{v_e}\frac{\omega}{k^2}e^{-\frac{1}{2}\left(\frac{\omega}{kv_e}\right)^2}e^{-\frac{1}{2}\left(\frac{k}{k_{\text{B}}}\right)^2}\sinh\left(\frac{\omega}{k_{\text{B}}v_e}\right) \quad (3.5)$$

$$\Im\{\mathcal{G}^{\text{qu}}(k,\omega)\} = \frac{k_{\text{B}}}{\sqrt{\pi}v_e}\frac{\omega}{k^2}\left[D\left(\frac{\omega}{\sqrt{2}kv_e}+\frac{k}{\sqrt{2}k_{\text{B}}}\right)-D\left(\frac{\omega}{\sqrt{2}kv_e}-\frac{k}{\sqrt{2}k_{\text{B}}}\right)\right] \quad (3.6)$$

$$\Re\{\epsilon^{\text{qu}}(k,i\omega)\} = 1 - \frac{k_{\text{B}}n_e^0\Phi_{ee}(k)}{\sqrt{2}m_ev_e^2k}\left[D\left(\frac{\omega}{\sqrt{2}kv_e}+\frac{k}{\sqrt{2}k_{\text{B}}}\right)-D\left(\frac{\omega}{\sqrt{2}kv_e}-\frac{k}{\sqrt{2}k_{\text{B}}}\right)\right] \quad (3.7)$$

$$\Im\{\epsilon^{\text{qu}}(k,i\omega)\} = \sqrt{\frac{\pi}{2}}\frac{k_{\text{B}}n_e^0\Phi_{ee}(k)}{m_ev_e^2k}e^{-\frac{1}{2}\left(\frac{\omega}{kv_e}\right)^2}e^{-\frac{1}{2}\left(\frac{k}{k_{\text{B}}}\right)^2}\sinh\left(\frac{\omega}{k_{\text{B}}v_e}\right) \quad (3.8)$$

$$\Re\{\mathcal{G}^{\text{cl}}(k,\omega)\} = \left(\frac{\omega}{kv_e}\right)^2e^{-\frac{1}{2}\left(\frac{\omega}{kv_e}\right)^2} \quad (3.9)$$

$$\Im\{\mathcal{G}^{\text{cl}}(k, \omega)\} = \sqrt{\frac{2}{\pi}} \frac{\omega}{kv_e} \left[1 - \sqrt{2} \frac{\omega}{kv_e} D\left(\frac{\omega}{\sqrt{2}kv_e}\right) \right] \quad (3.10)$$

$$\Re\{\epsilon^{\text{cl}}(k, i\omega)\} = 1 - \frac{n_e^0 \Phi_{ee}(k)}{m_e v_e^2} \left[1 - \sqrt{2} \frac{\omega}{kv_e} D\left(\frac{\omega}{\sqrt{2}kv_e}\right) \right] \quad (3.11)$$

$$\Im\{\epsilon^{\text{cl}}(k, i\omega)\} = \sqrt{\frac{\pi}{2}} \frac{n_e^0 \Phi_{ee}(k)}{m_e v_e^2} \frac{\omega}{kv_e} e^{-\frac{1}{2}\left(\frac{\omega}{kv_e}\right)^2} . \quad (3.12)$$

The interaction potentials $\Phi_{ei}(k)$ and $\Phi_{ee}(k)$ as Dawsons Integral $D(x)$ are given by

$$\Phi_{ei}(k) = \frac{Ze^2}{\epsilon_0} \frac{1}{k^2} , \quad \Phi_{ee}(k) = -\frac{e^2}{\epsilon_0} \frac{1}{k^2} , \quad D(x) = e^{-x^2} \int_0^x dt e^{t^2} .$$

We normalize the wavenumber and the frequency according to

$$k \rightarrow k/k_D = k\lambda_D = kv_e/\omega_p , \quad \omega_0 \rightarrow \omega_0/\omega_p , \quad \omega_p^2 = n_e^0 e^2 / \epsilon_0 m_e , \quad v_{os} = \omega_0 r_{os}$$

and multiply by the ion density $n_i^0 = n_e^0/Z$ (quasi neutrality). Because of the comparison to the literature the function \mathcal{G} is substituted by $\Xi = \sqrt{\frac{\pi}{2}} \frac{\mathcal{G}}{k\omega}$. The cycle-averaged absorbed energy *density* is then given by

$$\overline{\dot{\mathcal{E}}_{\text{RPA}}} = -\frac{Zm_e\omega_p^4\omega_0^2}{\pi^2 v_{os}} \int_0^\infty \frac{dk}{k} \sum_{l=1}^\infty l \Re\left\{ \frac{\Xi(k, l\omega_0)}{\epsilon(k, il\omega_0)} \right\} \int_0^{\frac{kv_{os}}{\omega_0 v_e}} d\xi J_l^2(\xi) . \quad (3.13)$$

The classical and the quantum kinetic expressions only differ by the functions $\epsilon(k, i\omega)$ and $\Xi(k, \omega)$.

3.1.1 The long-wavelength approximation (LWA) and a remark on the literature

In the literature the term $\Xi(k, \omega)$ in Eq. (3.13) generally does not occur. The reason for this is that the current density is treated in dipole approximation, the same as the so called 'straight orbit assumption', which can be done in the LWA limit $k \rightarrow 0$. In detail this occurs in our framework if we set $\vec{r}_e = (t - \tau)\vec{p}_e/m_e$ in Eq. (3.1). In the work of Hazak *et al.* [11] the corresponding term also appears and is treated in the LWA limit, that is in our notation $\Xi \approx -i$ for $k \ll 1$. Figure 3.1(a) shows the real and imaginary part of $\Xi(k, \omega)$. We realize that the LWA limit is fulfilled only up to $k \approx 0.2$, which is a very narrow region. So, this approximation seems to be poor. Nevertheless, what we are really looking for is a good approximation for the numerator of

$$\Re\left\{ \frac{\Xi}{\epsilon} \right\} = \frac{\Re\{\Xi\}\Re\{\epsilon\} + \Im\{\Xi\}\Im\{\epsilon\}}{\Re^2\{\epsilon\} + \Im^2\{\epsilon\}} = -\frac{\Gamma(k, \omega)}{\Re^2\{\epsilon\} + \Im^2\{\epsilon\}} .$$

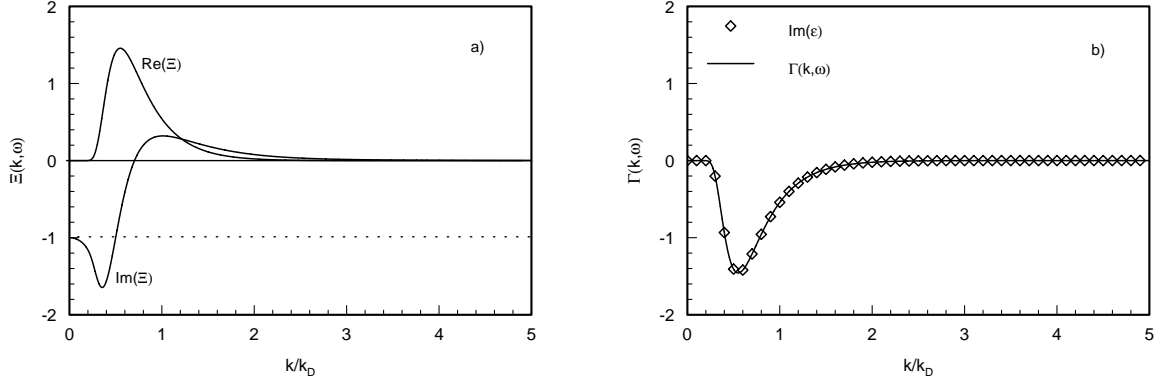


Figure 3.1: a) The real and imaginary parts of the function $\Xi(k, \omega)$ for $\omega = \omega_p$ and $k_B = k_D$; the LWA limit $\Im \Xi = -1$ is reached at $k = 0$. b) The imaginary part of the dielectric function $\epsilon(k, i\omega)$ as well as the function $\Gamma(k, \omega)$ also for $\omega = \omega_p$ and $k_B = k_D$.

Looking at Fig. 3.1(b) we recognize that the numerator $\Gamma(k, \omega)$ is best approximated by the imaginary part of the dielectric function $\Im \epsilon(k, i\omega)$ and this reproduces the results from the literature. But, the current density as the *time-dependent* absorption is not well approximated by the LWA limit.

We close this section with our final expression for the *cycle-averaged absorbed energy density*:

$$\overline{\mathcal{E}_{\text{RPA}}} = \frac{Z m_e \omega_p^4 \omega_0^2}{\pi^2 v_{\text{os}}} \int_0^\infty \frac{dk}{k} \sum_{l=1}^\infty l \frac{\Im \epsilon(k, i l \omega_0)}{|\epsilon(k, i l \omega_0)|^2} \int_0^{\frac{k v_{\text{os}}}{\omega_0 v_e}} d\xi J_l^2(\xi) . \quad (3.14)$$

3.2 The ballistic treatment

This model is based on a work of P. Mulser [16]. The impressive simplicity of this model leads to analytical expressions for the *time-dependent collision frequency* in an immediate way which where missing in the literature so far.

The collision frequency is calculated on the basis of a ballistic interaction model. Using the electron-ion scattering cross section the two-body interaction between one electron and one test ion is treated to all orders. The collision is treated as an instantaneous event not including the external field of the laser. The collective interaction of the electron is not calculated self-consistently, it is suggested by a screening length only.

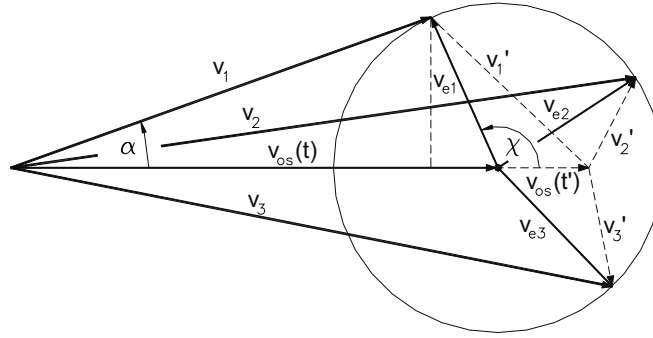


Figure 3.2: Isotropic electron distribution $f(v_e)$. The resultant velocities $\mathbf{v} = \mathbf{v}_{os} + \mathbf{v}_e$ consist of all types of vectors $\mathbf{v}_i, \mathbf{v}_i'$ indicated in the Figure for two oscillation velocities $\mathbf{v}_{os}(t)$ and $\mathbf{v}_{os}(t')$. The momentum losses \mathbf{p} form the angles α with \mathbf{v}_{os} ; the average loss $\langle \mathbf{p} \rangle$ is directed along \mathbf{v}_{os} .

One electron of the statistical ensemble possesses the velocity $\mathbf{v}(t) = \mathbf{v}_{os}(t) + \mathbf{v}_e$. During one collision with an ion of charge Ze the electron is deflected by an angle ϑ . The momentum change in direction of \mathbf{v} is $\Delta \mathbf{p}_\vartheta = \mathbf{v}(1 - \cos \vartheta)$. The differential cross section σ_Ω and the impact parameter for perpendicular deflection are given by

$$\sigma_\Omega = \frac{b_\perp^2}{4 \sin^4 \frac{\vartheta}{2}}, \quad b_\perp = \frac{Ze^2}{4\pi\epsilon_0 m_e v^2} = 7 \frac{Z}{E[eV]} [\text{\AA}], \quad \tan \frac{\vartheta}{2} = \frac{b_\perp}{b}. \quad (3.15)$$

Integration of $\Delta \mathbf{p}_\vartheta$ over the total cross section $\sigma = \pi b_{\max}^2$ results in

$$\begin{aligned} \Delta \mathbf{p} &= m_e \mathbf{v} \frac{b_\perp^2}{\sigma} \int_{\vartheta=\varepsilon}^{\pi-\varepsilon} \frac{(1 - \cos \vartheta) \sin \vartheta}{4 \sin^4 \frac{\vartheta}{2}} d\vartheta d\varphi \\ &= 4\pi m_e \mathbf{v} \frac{b_\perp^2}{\sigma} \int_{b_{\min}}^{b_{\max}} \frac{1}{1 + \left(\frac{b_\perp}{b}\right)^2} \frac{db}{b} \\ &= 4\pi m_e \mathbf{v} \frac{b_\perp^2}{\sigma} \frac{1}{2} \ln \frac{b_{\max}^2 + b_\perp^2}{b_{\min}^2 + b_\perp^2} \end{aligned} \quad (3.16)$$

$$= 4\pi m_e \mathbf{v} \frac{b_{\perp}^2}{\sigma} \ln \Lambda .$$

$\ln \Lambda$ denotes the so called *Coulomb Logarithm*. The lengths b_{\max} and b_{\min} herein are identified by the screening length and the De Broglie wavelength. The upper cut-off b_{\max} is necessary to avoid a logarithmic divergency for large b . In Sections 3.3.2 and 3.3.4 these lengths will be analyzed based on the kinetic treatment.

Notice that the collision parameter b_{\perp} for perpendicular deflection is an inherent quantity for the Coulomb collision and not a cut-off.

The momentum loss per unit time is $\dot{\mathbf{p}} = \sigma n_i |\mathbf{v}| \Delta \mathbf{p}$,

$$\dot{\mathbf{p}} = -m_e \nu_{ei}(\mathbf{v}) \mathbf{v} = -\frac{K}{v^3} \mathbf{v}, \quad K = \frac{Z^2 e^4 n_i}{4\pi \varepsilon_0^2 m_e} \ln \Lambda. \quad (3.17)$$

By the first equation the collision frequency $\nu_{ei}(\mathbf{v})$ is defined. To obtain the ensemble average of the momentum loss $\langle \dot{\mathbf{p}} \rangle$ we have to average \mathbf{v}/v^3 over the thermal velocities \mathbf{v}_e . An isotropic electron distribution function is assumed $f(v_e)$. The velocity \mathbf{v} consists of all vector sums as sketched in Fig. 3.2. The momentum loss $\dot{\mathbf{p}}$ is parallel to \mathbf{v} , whereas the ensemble average points along \mathbf{v}_{os} . Determining the average of \mathbf{v}/v^3 is perfectly analogous to calculating the gravitational force of a spherical mass distribution on a point mass at distance R from its center. The Coulomb Logarithm is treated as a constant during the average. We obtain

$$\langle \dot{\mathbf{p}} \rangle = m_e \nu_{ei}(t) \mathbf{v}_{\text{os}} = K \frac{\mathbf{v}_{\text{os}}}{v_{\text{os}}^3} \int_0^{v_{\text{os}}} 4\pi v_e^2 f(v_e) dv_e .$$

The *time-dependent* collision frequency of the ensemble is defined by $\langle \nu_{ei}(\mathbf{v}) \mathbf{v} \rangle = \nu_{ei}(t) \langle \mathbf{v} \rangle = \nu_{ei}(t) \mathbf{v}_{\text{os}}$ and results in

$$\nu_{ei}(t) = \frac{K}{m_e v_{\text{os}}^3(t)} \int_0^{v_{\text{os}}} 4\pi v_e^2 f(v_e) dv_e . \quad (3.18)$$

Taking a Maxwell distribution

$$f_M = (2\pi v_{\text{th}}^2)^{-3/2} e^{-\frac{v_e^2}{2v_{\text{th}}^2}}$$

we obtain

$$\nu_{ei}(t) = \frac{K}{m_e v_{\text{os}}^3(t)} \left[\text{erf} \left(\frac{v_{\text{os}}(t)}{\sqrt{2} v_{\text{th}}} \right) - \frac{2}{\sqrt{\pi}} \frac{v_{\text{os}}(t)}{\sqrt{2} v_{\text{th}}} e^{-\frac{v_{\text{os}}^2(t)}{2v_{\text{th}}^2}} \right] . \quad (3.19)$$

The energy absorption is related to the *time averaged* collision frequency by

$$m_e \overline{\nu_{ei} \mathbf{v}_{\text{os}}^2} = m_e \overline{\nu_{ei}} \overline{\mathbf{v}_{\text{os}}^2} = 2 \overline{\nu_{ei}} \overline{E_{\text{kin}}} .$$

Thus, for the time averaged energy absorption density we find

$$\boxed{\overline{\mathcal{E}} = 2n_e \overline{\nu_{ei}} \overline{E_{\text{kin}}} = Z\omega_p^4 m_e \ln \Lambda \overline{\frac{1}{v_{\text{os}}(t)} \int_0^{v_{\text{os}}(t)} v_e^2 f_M(v_e) dv_e} .} \quad (3.20)$$

3.3 A combined model for collisional absorption

The kinetic calculation of the absorption done in Sec. 3.1 includes screening and quantum effects in a self-consistent manner, but it is limited to first order in the electron-ion interaction. In contrast, in the ballistic model the electron-ion collisions are calculated exactly in each order of the interaction, but cut-offs have to be introduced from outside to incorporate screening and quantum effects. In the following sections we shall join both treatments to get a *combined* model, avoiding in this way the inherent approximations: i) first order electron-ion interaction only, ii) the artificial introduction of cut-offs. (See also the discussion in Sec. 2.1.4.)

3.3.1 The connection between the kinetic and the ballistic treatment

In the following the symbol v_{th} denotes the thermal velocity of the electrons and \hat{v}_{os} the amplitude of the electron oscillation velocity. The wavenumber k is normalized to $k_D = \lambda_D^{-1}$, the inverse thermal Debye length, and the laser frequency ω_0 is normalized to the plasma frequency ω_p .

From the *kinetic* treatment of the absorption we found, Eq. (3.14),

$$\overline{\dot{\mathcal{E}}_{\text{RPA}}} = \frac{Zm_e\omega_p^4}{\pi^2\hat{v}_{\text{os}}} \int_0^\infty \frac{dk}{k} F\left(k, \omega_0, \frac{\hat{v}_{\text{os}}}{v_{\text{th}}}\right) \quad (3.21)$$

with the integral kernel

$$F\left(k, \omega_0, \frac{\hat{v}_{\text{os}}}{v_{\text{th}}}\right) = \omega_0^2 \sum_{l=1}^{\infty} l \frac{\Im\epsilon(k, il\omega_0)}{|\epsilon(k, il\omega_0)|^2} \int_0^{\frac{k\hat{v}_{\text{os}}}{\omega_0 v_{\text{th}}}} d\xi J_l^2(\xi) \quad (3.22)$$

From the *ballistic* treatment we got Eq. (3.20),

$$\begin{aligned} \overline{\dot{\mathcal{E}}_{\text{ball}}} &= \frac{Zm_e\omega_p^4}{\pi^2\hat{v}_{\text{os}}} \ln\Lambda G\left(\frac{\hat{v}_{\text{os}}}{v_{\text{th}}}\right) \\ \ln\Lambda &= \frac{1}{2} \ln \frac{b_{\text{max}}^2 + b_{\perp}^2}{b_{\text{min}}^2 + b_{\perp}^2} \end{aligned} \quad (3.23)$$

where we have introduced the abbreviation

$$G\left(\frac{\hat{v}_{\text{os}}}{v_{\text{th}}}\right) = \pi^2\hat{v}_{\text{os}} \frac{1}{v_{\text{os}}(t)} \int_0^{v_{\text{os}}(t)} v_e^2 f_M(v_e) dv_e \quad (3.24)$$

For the moment, setting the dielectric function $\epsilon = \epsilon^{\text{cl}}$, Eqs. (3.11) and (3.12), we restrict the function F to the classical regime. The inclusion of quantum effects will follow in Sec. 3.3.4.

The integral kernel F is a very complicated function. It is difficult to obtain analytically F

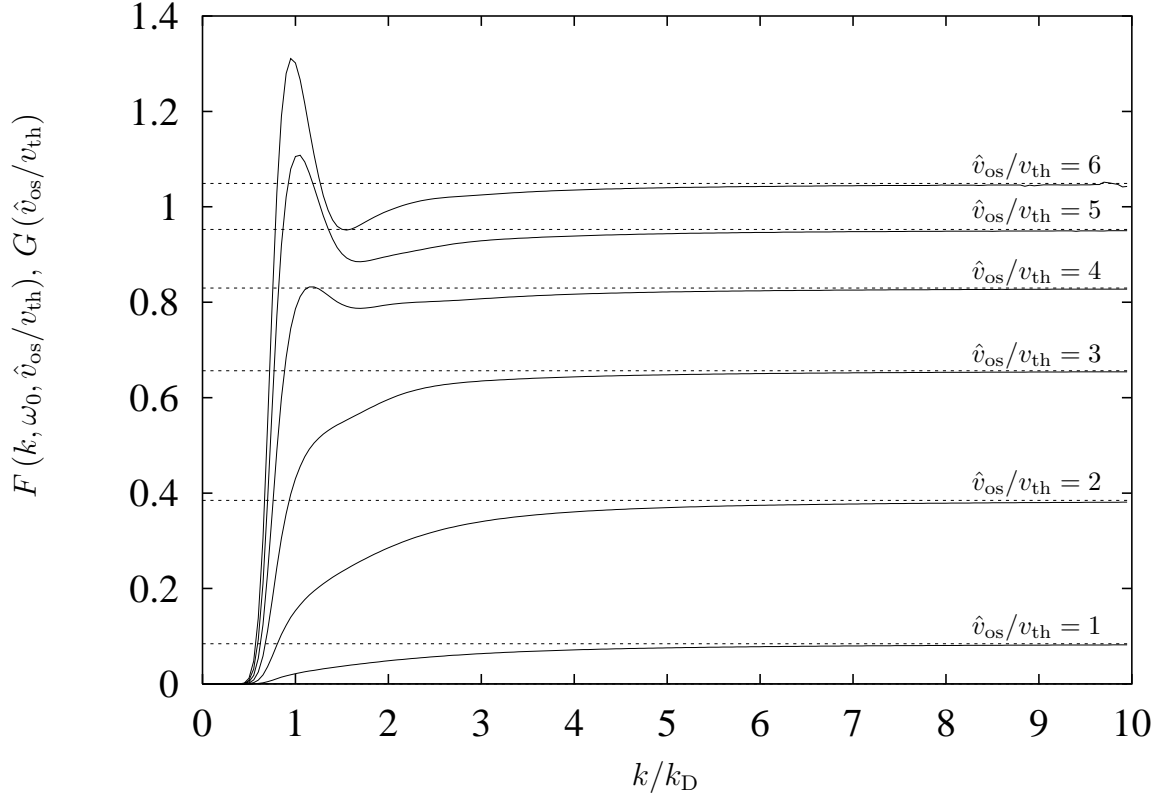


Figure 3.3: The kinetic integral kernel F (solid, eq. (3.22)) and the ballistic function G (dashed, Eq. (3.24)) for $\omega_0/\omega_p = 2$ and $1 \leq \hat{v}_{os}/v_{th} \leq 6$. The kernel F asymptotically reaches the function G for large wavenumbers k . For $\hat{v}_{os}/v_{th} \rightarrow 0$ the functions F and G go to zero for all k/k_D .

in dependence of k and v_{os}/v_{th} . Therefore, in Fig. 3.3 F is plotted numerically over k for a wide range of \hat{v}_{os} , namely $1 \leq \hat{v}_{os}/v_{th} \leq 6$. The ratio ω_0/ω_p is set equal to 2. Now, when evaluating numerically G the most remarkable result is obtained that, latest from $k/k_D = 3$ the function G represents an excellent approximation of F , as seen from Fig. 3.3. From the numerical analysis we deduce the asymptotic equivalence

$$\lim_{k \rightarrow \infty} F\left(k, \omega_0, \frac{\hat{v}_{os}}{v_{th}}\right) = G\left(\frac{\hat{v}_{os}}{v_{th}}\right) \quad (3.25)$$

which connects the kinetic absorption rate Eq. (3.21) and the absorption rate calculated by the ballistic model Eq. (3.23).

This asymptotic equivalence is the salient point of the present work. It is the foundation for further analytical simplifications of the absorption rate which otherwise are very hard to achieve. In fact, as we shall see in a moment, it introduces the concept of the Coulomb Logarithm into the kinetic treatment, and by choosing the latter appropriately the equiva-

lence between the ballistic and the kinetic model can be shown.

The fact, that the integral kernel F becomes constant for large wavenumbers, leads, in the classical case, to the well known logarithmic divergence in Eq. (3.21). This divergence occurs because of the first order Born approximation which only describes weak collisions correctly. The inclusion of strong binary collisions, Sec. 3.3.3, as well as quantum effects, Sec. 3.3.4, will remove this divergence. It is standard to avoid the divergence by replacing the upper limit of the integral with a upper cut-off k_{\max} .

The decomposition of the function F into a product of a rectangular Theta-function $\Theta(k - k_{\min})$ and the function G in such a way that the areas in Fig. 3.3 become equal immediately leads to the Coulomb Logarithm $\ln \Lambda$ of the ballistic model, Eq. (3.23), when set $b_{\perp} = 0$ (first order Born approximation):

$$\begin{aligned} \int_0^{k_{\max}} \frac{dk}{k} F\left(k, \omega_0, \frac{\hat{v}_{\text{os}}}{v_{\text{th}}}\right) &= \int_0^{k_{\max}} \frac{dk}{k} G\left(\frac{\hat{v}_{\text{os}}}{v_{\text{th}}}\right) \Theta(k - k_{\min}) \\ &= G\left(\frac{\hat{v}_{\text{os}}}{v_{\text{th}}}\right) \ln \frac{k_{\max}}{k_{\min}} = G\left(\frac{\hat{v}_{\text{os}}}{v_{\text{th}}}\right) \ln \frac{b_{\max}}{b_{\min}} \\ \ln \Lambda &= \ln \frac{b_{\max}}{b_{\min}} . \end{aligned} \quad (3.26)$$

The lower cut-off $k_{\min} = b_{\max}^{-1}$ is identified with the inverse screening length of the ion potential. In the ballistic model this length is introduced from outside. By the above equations we are able to determine the screening length self-consistently which is done in the next section.

3.3.2 The screening length

For small wavenumbers the asymptotic equality Eq. (3.25) is not fulfilled. The kinetic integral kernel F decreases for $k < 4k_D$ because of the screening of the ion potential by the electrons, see Fig. 3.3. For a plasma in thermal equilibrium the effective screening length is given by the Debye length $\lambda_D = k_D^{-1} = v_{\text{th}}/\omega_p$. Now, in the presence of a strong laser field due to the electron oscillation the screening length is expected to contain a dynamical part which should scale as $\hat{v}_{\text{os}}/\max(\omega_0, \omega_p)$ [15].

This dynamical screening length is the inverse k_{\min} introduced in the previous section. It is determined self-consistently by comparing the integrals

$$\int_0^{k_0} \frac{dk}{k} F\left(k, \omega_0, \frac{\hat{v}_{\text{os}}}{v_{\text{th}}}\right) = \int_0^{k_0} \frac{dk}{k} G\left(\frac{\hat{v}_{\text{os}}}{v_{\text{th}}}\right) \Theta(k - k_{\min}).$$

Whatever the value of k_0 is, as long as k_0 is in the range of the asymptotic, $F(k_0) = G$, the inverse screening length k_{\min} does not depend on k_0 .

The kinetic inverse screening length becomes

$$k_{\min} = k_0 \exp\left(-\int_0^{k_0} \frac{dk}{k} \frac{F}{G}\right) . \quad (3.27)$$

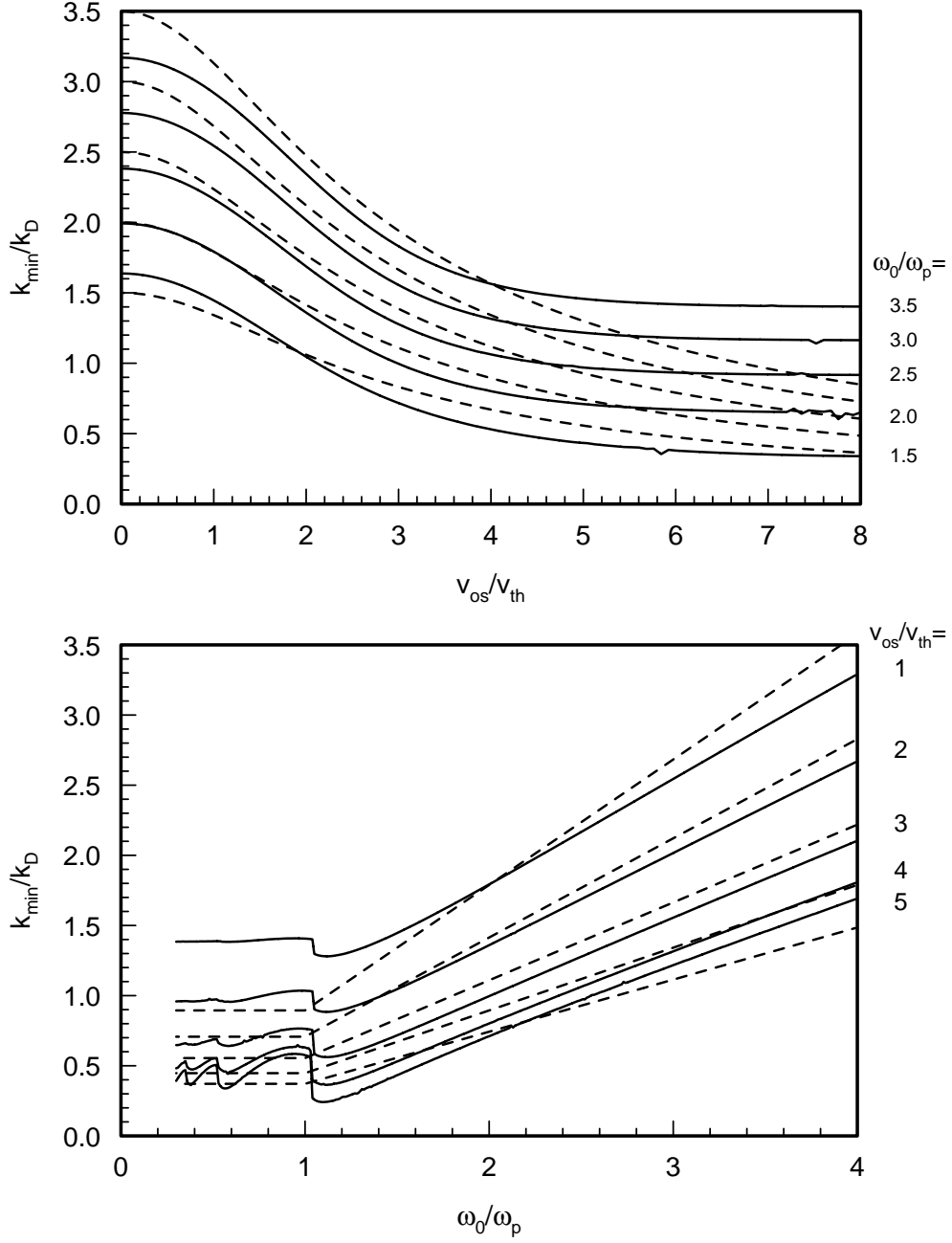


Figure 3.4: The inverse screening length k_{\min} (solid, eq. (3.27)) and the approximation (dashed, Eq. (3.28)) as a function of the electron oscillation velocity over the electron thermal velocity \hat{v}_{os}/v_{th} (top) and as a function of the laser frequency over the plasma frequency ω_0/ω_p (bottom).

In Fig. 3.4 k_{\min} is plotted over $\hat{v}_{\text{os}}/v_{\text{th}}$ and ω_0/ω_p (solid lines). As a rough approximation for k_{\min} , similar to [16], we choose

$$k_{\min} \approx \left(\frac{\sqrt{\hat{v}_{\text{os}}^2/4 + v_{\text{th}}^2}}{\max(\omega_0, \omega_p)} \right)^{-1} \quad (3.28)$$

which ensures the expected asymptotic behavior as one of the four quantities goes to zero. The expression is also plotted in Fig. 3.4 (dashed lines). In contrast to [16] in the above expression for k_{\min} the oscillation term is changed empirically from $\hat{v}_{\text{os}}^2/2$ to $\hat{v}_{\text{os}}^2/4$ since this leads to a better agreement.

A so far unknown behavior of the dynamical screening length appears in the upper of Figs. 3.4: *the exact inverse screening length k_{\min}^{-1} saturates for large oscillation velocities* (solid lines) *in contrast to a decrease proportional to \hat{v}_{os}^{-1} which is expected from the literature.* This feature is not understood so far; however, an explanation is in progress. The ω_0/ω_p dependence is qualitatively as expected. Beside the saturation for large \hat{v}_{os} the approximation, Eq. (3.28), works quite well. Last but not least, because k_{\min}^{-1} enters only logarithmically in the absorption rate the deviations are reduced.

3.3.3 Strong two-body collisions

As mentioned in the beginning of this section, our kinetic approach is not able to handle strong two-body collisions because of the first order Born approximation. However, the ballistic treatment is able. To include strong two-body collisions in the kinetic treatment one has to calculate, in addition to the RPA-diagrams (Eq. (2.12)), the infinite series of ladder-diagrams, Eq. (2.8). Nevertheless, also for this simplified approach a complete analytical solution is not accessible because of the time varying electric field of the laser. The kinetic model includes the laser field exactly for the weak collisions. During a strong two-body collision the Coulomb force dominates the interaction with the electric field of the laser. Therefore, it is sufficient to take account for the electric field in the velocity of the impinging electron as done by the ballistic model.

Let us rewrite the absorption rate from the ballistic model, Eq. (3.23), using the integral notation for the Coulomb Logarithm, Eq. (3.16). Therein b_{\min} is set zero because it is an artificial cut-off which is not part of the kinetic treatment:

$$\begin{aligned} \overline{\dot{\mathcal{E}}_{\text{ball}}} &= \frac{Zm_e\omega_p^4}{\pi^2\hat{v}_{\text{os}}} G\left(\frac{\hat{v}_{\text{os}}}{v_{\text{th}}}\right) \int_0^{b_{\max}} \frac{1}{1 + \left(\frac{b_{\perp}}{b}\right)^2} \frac{db}{b} \quad \Big|_{k=b^{-1}} \\ &= \frac{Zm_e\omega_p^4}{\pi^2\hat{v}_{\text{os}}} G\left(\frac{\hat{v}_{\text{os}}}{v_{\text{th}}}\right) \int_{k_{\min}}^{\infty} \frac{1}{1 + (kb_{\perp})^2} \frac{dk}{k} . \end{aligned}$$

Using the results from Sections 3.3.1 and 3.3.2 the kinetic absorption rate becomes

$$\overline{\dot{\mathcal{E}}_{\text{RPA}}} = \frac{Zm_e\omega_p^4}{\pi^2\hat{v}_{\text{os}}} \int_0^{\infty} \frac{dk}{k} F\left(k, \omega_0, \frac{\hat{v}_{\text{os}}}{v_{\text{th}}}\right)$$

$$= \frac{Zm_e\omega_p^4}{\pi^2\hat{v}_{os}} G\left(\frac{\hat{v}_{os}}{v_{th}}\right) \int_{k_{min}}^{\infty} \frac{dk}{k} .$$

Comparing the above integrals inside the ballistic and the kinetic expressions we observe the additional factor $(1 + (kb_{\perp})^2)^{-1}$ in the ballistic case, which is the only difference. This factor has its seeds in the strong two-body collisions; if we take the limit $b_{\perp} \rightarrow 0$ we recover the first order Born approximation. As outlined above the ballistic and the classical dielectric model coincide for weakly bent orbits if the Coulomb logarithm is defined properly. Furthermore, in the ballistic model the contribution of the strongly bent orbits is correctly included if the interaction is an unshielded Coulomb potential, or, in other words, when $b_{\perp} \ll \lambda_D$. Since these orbits are also solutions of the Vlasov equation when $b_{\perp} \ll \lambda_D$ we have proved that the kinetic integral, Eq. (3.21), is to be regularized by b_{\perp} in order to treat close encounters. The absorption rate from this combined approach takes the form

$$\bar{\mathcal{E}} = \frac{Zm_e\omega_p^4}{\pi^2\hat{v}_{os}} \int_0^{\infty} \frac{dk}{k} \frac{1}{1 + (kb_{\perp})^2} F\left(k, \omega_0, \frac{\hat{v}_{os}}{v_{th}}\right) . \quad (3.29)$$

3.3.4 Inclusion of quantum effects

The choice of the quantum kinetic dielectric function, Eq. (3.7) and Eq. (3.8), within the integral kernel F , Eq. (3.21), leads to the quantum kinetic expression for the absorption. The major differences to the classical integral kernel appear in the numerator of F due to the imaginary part of the dielectric function. The quantum expression contains a Gaussian decrease for large ratios k/k_B as well as a sinh-dependency of the frequency. At first glance, it seems to be surprising that only the thermal De Broglie wavenumber appears, which we defined in Appendix B as $k_B = (\hbar/2m_e v_{th})^{-1}$. We would expect that due to the oscillatory motion of the electrons also a term depending on the oscillation velocity should occur. And indeed, the physical intuition is right! The numerical analysis of F shows that the oscillation velocity enters the De Broglie wavenumber due to the sinh-term inside the imaginary part of the quantum kinetic dielectric function, $\sinh(l\omega_0/k_B v_{th})$. This term rescales the De Broglie wavenumber by an average velocity of about $\sqrt{\hat{v}_{os}^2/4 + v_{th}^2}$. Analytically the meaning of this term is not obvious because it does not depend on \hat{v}_{os} . The only coupling to \hat{v}_{os} occurs according to the summation over the integrals of Bessel functions where \hat{v}_{os} appears in the upper limit of the integrals. The numerical analysis shows that neglecting the sinh-term only the thermal De Broglie wavenumber occurs.

In Fig. 3.5 the full quantum kinetic kernel

$$F_{qu}\left(k, \omega_0, \frac{\hat{v}_{os}}{v_{th}}\right) = \omega_0^2 \sum_{l=1}^{\infty} l \frac{\Im \epsilon^{qu}(k, il\omega_0)}{|\epsilon^{qu}(k, il\omega_0)|^2} \int_0^{\frac{k\hat{v}_{os}}{\omega_0 v_{th}}} d\xi J_l^2(\xi) , \quad (3.30)$$

the classical one

$$F_{cl}\left(k, \omega_0, \frac{\hat{v}_{os}}{v_{th}}\right) = \omega_0^2 \sum_{l=1}^{\infty} l \frac{\Im \epsilon^{cl}(k, il\omega_0)}{|\epsilon^{cl}(k, il\omega_0)|^2} \int_0^{\frac{k\hat{v}_{os}}{\omega_0 v_{th}}} d\xi J_l^2(\xi) \quad (3.31)$$

and the approximation

$$F_{\text{av}} \left(k, \omega_0, \frac{\hat{v}_{\text{os}}}{v_{\text{th}}} \right) = e^{-\frac{1}{2} \left(\frac{k}{\langle k_{\text{B}} \rangle} \right)^2} F_{\text{cl}} \left(k, \omega_0, \frac{\hat{v}_{\text{os}}}{v_{\text{th}}} \right) \quad (3.32)$$

are compared to each other. In the latter we have introduced the *mean* De Broglie wavenumber

$$\langle k_{\text{B}} \rangle = \left(\frac{\hbar}{2m_e \sqrt{\hat{v}_{\text{os}}^2/4 + v_{\text{th}}^2}} \right)^{-1}. \quad (3.33)$$

The approximation is quite well fulfilled for the whole parameter region. This is a very useful result and makes analytic approximations for the absorption quite easy. Note that only taking into account the thermal De Broglie wavenumber ($F = F_{\text{th}}$) and neglecting the discussed sinh-term, underestimates the integral kernel for $v_{\text{os}} > v_{\text{th}}$, Fig. 3.5 c) and d).

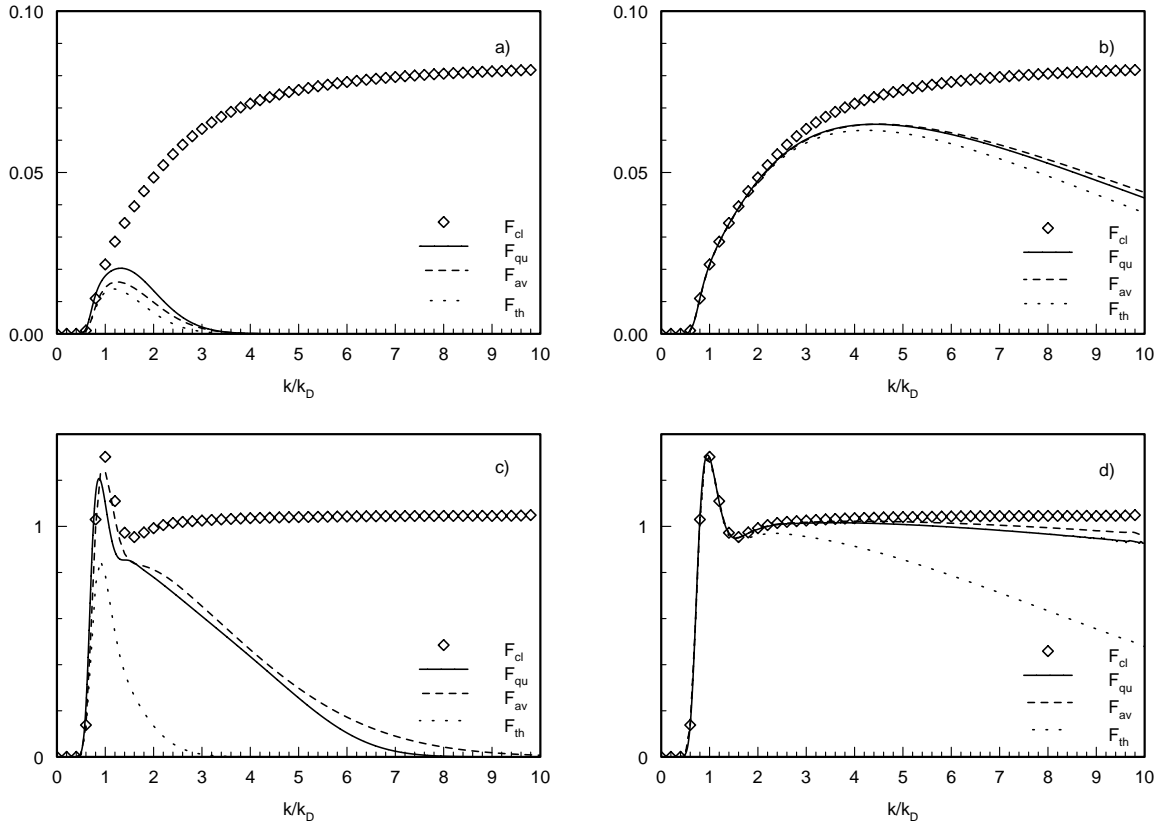


Figure 3.5: Plot of the integral kernel, Eq. (3.22), in the classical case F_{cl} , in the quantum regime F_{qu} , the approximation F_{av} , and the approximation F_{th} which contains the thermal De Broglie wavenumber only; $\omega_0 = 2\omega_p$; a) $k_{\text{B}} = k_{\text{D}}$, $\hat{v}_{\text{os}} = v_{\text{th}}$; b) $k_{\text{B}} = 8k_{\text{D}}$, $\hat{v}_{\text{os}} = v_{\text{th}}$; c) $k_{\text{B}} = k_{\text{D}}$, $\hat{v}_{\text{os}} = 6v_{\text{th}}$; d) $k_{\text{B}} = 8k_{\text{D}}$, $\hat{v}_{\text{os}} = 6v_{\text{th}}$. In all cases F_{av} agrees well with the correct expression F_{qu} when $\langle k_{\text{B}} \rangle$ is chosen as indicated by Eq. (3.33).

3.3.5 The combined absorption result

The combination of the results Eq. (3.29) and Eq. (3.32) leads us to the expression

$$\bar{\mathcal{E}} = \frac{Zm_e\omega_p^4}{\pi^2\hat{v}_{os}} \int_0^\infty \frac{dk}{k} \frac{e^{-\frac{1}{2}\left(\frac{k}{\langle k_B \rangle}\right)^2}}{1+(kb_\perp)^2} F_{cl}\left(k, \omega_0, \frac{\hat{v}_{os}}{v_{th}}\right) .$$

Again we use the asymptotic congruence of the ballistic with the kinetic model, Eq. (3.25), and write the k -dependence of the function F_{cl} as a theta function $\Theta(k - k_{min})$ where the inverse dynamical screening length k_{min} is determined by Eq. (3.27). The resultant k -integral $\ln \Lambda_G$,

$$\ln \Lambda_G = \int_{k_{min}}^\infty \frac{dk}{k} \frac{e^{-\frac{1}{2}\left(\frac{k}{\langle k_B \rangle}\right)^2}}{1+(kb_\perp)^2}$$

is solvable [20] and defines a *generalized Coulomb Logarithm* $\ln \Lambda_G$ expressed by a difference of exponential-integrals of the first kind [$\lambda_B = \langle k_B \rangle^{-1}$, $b_{max} = k_{min}^{-1}$]:

$$\boxed{\ln \Lambda_G = \frac{1}{2} \left[E_1 \left(\frac{1}{2} \left(\frac{\lambda_B}{b_{max}} \right)^2 \right) - e^{\frac{1}{2} \left(\frac{\lambda_B}{b_\perp} \right)^2} E_1 \left(\frac{1}{2} \left(\frac{\lambda_B}{b_{max}} \right)^2 + \frac{1}{2} \left(\frac{\lambda_B}{b_\perp} \right)^2 \right) \right]} . \quad (3.34)$$

This Coulomb Logarithm does never become negative, in contrast to the standard expression of $\ln \Lambda$ from Eq. (3.26), since the integrand is always positive. The problem of a negative Coulomb Logarithm, often noticed in the literature, does not occur.

For the time averaged absorption rate we end up with

$$\boxed{\bar{\mathcal{E}} = Zm_e\omega_p^4 \ln \Lambda_G \overline{\frac{1}{v_{os}(t)} \int_0^{v_{os}(t)} v_e^2 f_M(v_e) dv_e}} . \quad (3.35)$$

For the velocity dependence of the parameter for perpendicular deflection b_\perp , Eq. (3.15), we use the $\hat{v}_{os}^2/4 + v_{th}^2$ term by analogy to the velocity dependence of the average De Broglie length. From the ballistic model, Eq. (3.18) and Eq. (3.19), we get the cycle-averaged function in Eq. (3.35):

$$\overline{\frac{1}{v_{os}(t)} \int_0^{v_{os}(t)} v_e^2 f_M(v_e) dv_e} = \frac{\omega_0}{2\pi} \int_0^{\frac{2\pi}{\omega_0}} \frac{dt}{4\pi v_{os}(t)} \left[\operatorname{erf} \left(\frac{v_{os}(t)}{\sqrt{2}v_{th}} \right) - \frac{2}{\sqrt{\pi}} \frac{v_{os}(t)}{\sqrt{2}v_{th}} e^{-\frac{v_{os}^2(t)}{2v_{th}^2}} \right] \quad (3.36)$$

The numerical evaluation of this integral is quite simple. The result is shown in Fig. 3.6.

To confirm the correctness of the preceding analysis we look at the limit of the above generalized Coulomb Logarithm for a high energy plasma, that is, for small λ_B and b_\perp . Using for E_1 the expansion [21]

$$E_1(x) = -\gamma - \ln x - \sum_{n=1}^{\infty} \frac{(-1)^n x^n}{nn!} \quad \gamma = 0.5772156649... \text{ is Euler's constant,}$$

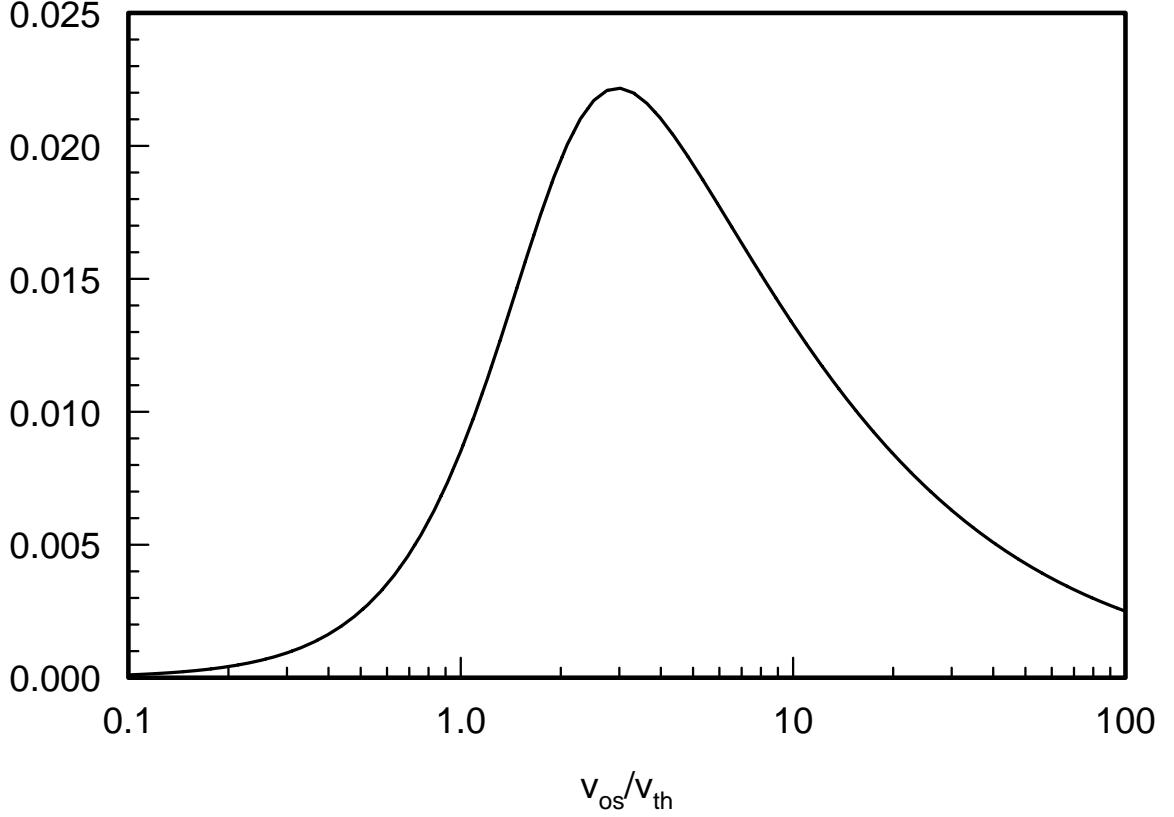


Figure 3.6: The function of Eq. (3.36) plotted over $\hat{v}_{\text{os}}/v_{\text{th}}$. The time dependent oscillation velocity is set as $v_{\text{os}}(t) = \hat{v}_{\text{os}} \cos \omega_0 t$. The result does not depend on the frequency of the oscillation nor on an arbitrary constant phase.

we find, in complete agreement to the ballistic model, the usual Coulomb Logarithm, Eq. (3.16), for $b_{\text{min}} = \lambda_B \rightarrow 0$:

$$\ln \Lambda_G \xrightarrow{\lambda_B \rightarrow 0} \frac{1}{2} \ln \left(1 + \frac{b_{\text{max}}^2}{b_{\perp}^2} \right) . \quad (3.37)$$

If b_{\perp} shrinks to zero we can use the relation [22]

$$\frac{1}{2} \ln \left(1 + \frac{2}{x} \right) < e^x E_1(x) < \ln \left(1 + \frac{1}{x} \right) \quad (x > 0)$$

which leads to

$$\ln \Lambda_G \xrightarrow{b_{\perp} \rightarrow 0} \frac{1}{2} E_1 \left(\frac{1}{2} \left(\frac{\lambda_B}{b_{\text{max}}} \right)^2 \right) \xrightarrow{\lambda_B \ll b_{\text{max}}} \ln \left(\sqrt{2} \frac{b_{\text{max}}}{\lambda_B} \right) - \frac{\gamma}{2} . \quad (3.38)$$

The latter limit for $\lambda_B \ll b_{\text{max}}$ is in agreement with results of Kull and Plagne [10].

Chapter 4

Results and Conclusion

For the comparison with the literature we relate the absorbed energy density rate to the electron-ion collision frequency according to the standard expression

$$\nu_{ei} = \frac{\bar{\mathcal{E}}}{2n_e \bar{E}_{\text{kin}}} = \frac{2\bar{\mathcal{E}}}{m_e n_e \hat{v}_{\text{os}}^2}$$

from the Drude model.

In Figure 4.1 the full quantum kinetic electron-ion collision frequency with and without inclusion of strong binary collisions is compared to the approximations given by the combined model. The full quantum solution is calculated only up to $\hat{v}_{\text{os}}/v_{\text{th}} = 10$ because of the large numerical effort involved; the numerical integration range in Eq. (3.29) is up to $k/k_{\text{D}} = 150$ and one has to add up about 500 Bessel functions for large values of k/k_{D} .

We have chosen the same parameters as shown by Bornath *et al.* [13, Fig. 1, 2]. Their results match exactly our ones in the case $b_{\perp} = 0$. Nevertheless, including strong binary collisions, that is $b_{\perp} \neq 0$, leads to a decrease in the collision frequency. This tendency is in agreement with the results of Gericke and Schlanges [19]. Including numerically the static T-Matrix - the sum of all ladder graphs - in the stopping power calculation of an ion-beam, they also find a decrease in the stopping power compared to the first order Born result. The approximation which takes into account the kinetic screening length, Eq. (3.35), is very successful. It becomes exact for values $\hat{v}_{\text{os}}/v_{\text{th}} > 3$. Using for the screening length the rough estimate Eq. (3.28) the approximation for the collision frequency fails for $\hat{v}_{\text{os}}/v_{\text{th}} < 4$ [Fig. 4.1, dotted line].

By the additional scale of b_{\perp} the collision frequency also changes its density dependence, as seen in Fig. 4.2. Due to the strong binary collisions the maximum of the electron-ion collision frequency is strongly shifted and reduced. At large densities the approximation Eq. (3.35) no longer fits the exact result. That is, because with increasing density the ratios $\lambda_{\text{B}}/\lambda_{\text{D}}$ as well as $b_{\perp}/\lambda_{\text{D}}$ become larger and one would have had to take into account these scales when calculating the screening length. In the upper of Fig. 4.2 the ratios take the values: $\lambda_{\text{B}}/\lambda_{\text{D}} = 0.007$ $b_{\perp}/\lambda_{\text{D}} = 0.012$ for $n_e = 10^{26}\text{m}^{-3}$; $\lambda_{\text{B}}/\lambda_{\text{D}} = 0.227$ $b_{\perp}/\lambda_{\text{D}} = 0.373$ for $n_e = 10^{29}\text{m}^{-3}$. The deviation becomes smaller with increasing \hat{v}_{os} and thus decreasing b_{\perp} , as seen from the lower of Fig. 4.2.

According to the Z dependency of b_{\perp} the collision frequency no longer depends linearly on the ion charge number, see Fig. 4.3. For the given values of $\hat{v}_{os}/v_{th} = 1.0$ (2.0) and $\omega_0/\omega_p = 5$ the collision frequency for $Z = 1$ scales as $\nu_{ei} \sim Z^{0.2}$ ($Z^{0.4}$). At $Z = 10$ this scaling changes to $\nu_{ei} \sim Z^{-0.8}$ ($Z^{-0.6}$). For larger energies at decreasing b_{\perp} the exponent will become 1. Again, this behavior according to the charge number Z is in agreement with the results of Gericke and Schlanges [19].

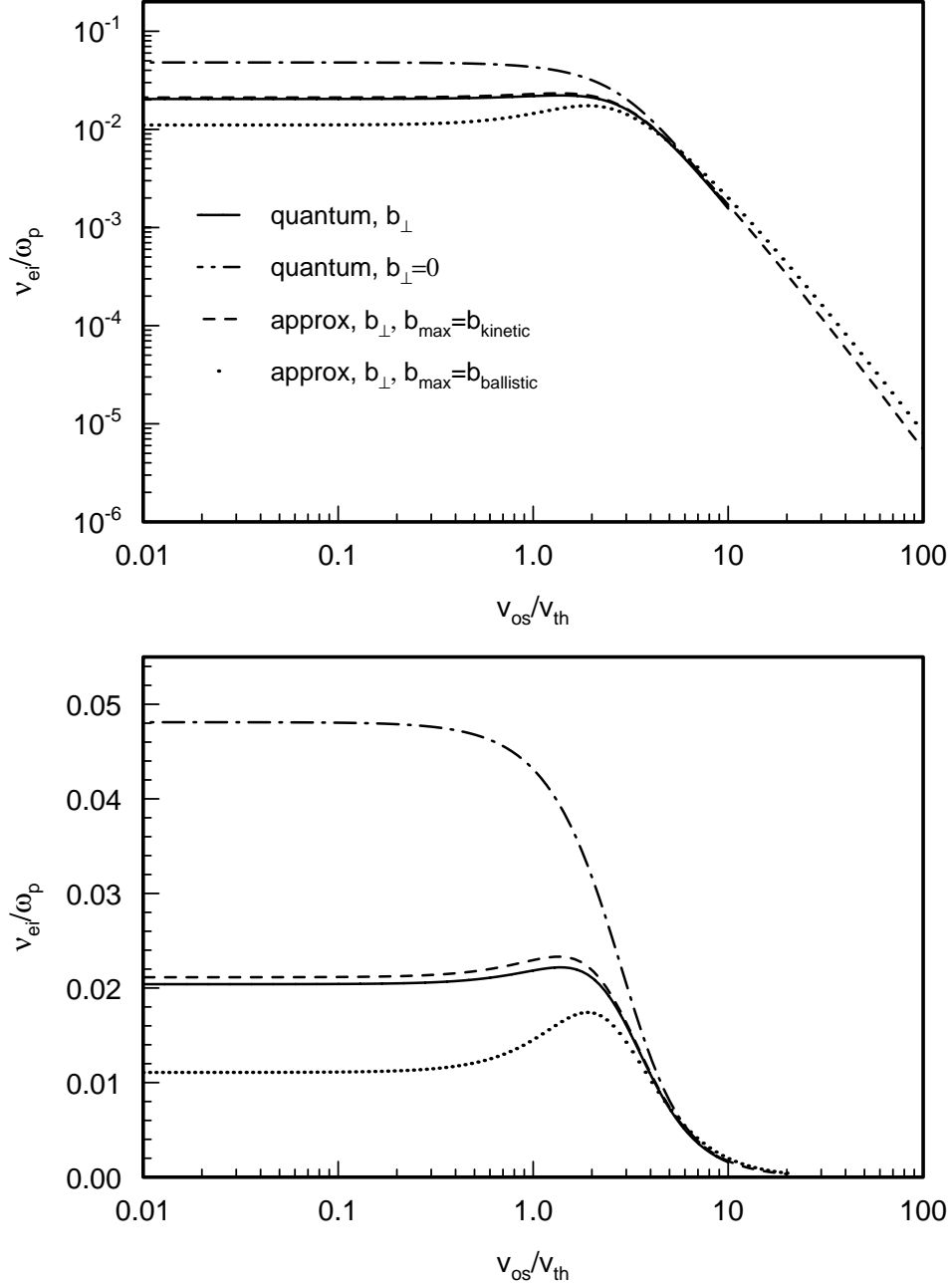


Figure 4.1: *Electron-ion collision frequency as a function of the oscillation velocity \hat{v}_{os} ; $Z = 1$, $n_e = 10^{28} \text{ m}^{-3}$, $T_e = 3 \cdot 10^5 \text{ K} = 25.85 \text{ eV}$, $\omega_0/\omega_p = 5$. The full quantum solution, Eq. (3.29), with and without b_{\perp} ; the approximation, Eq. (3.35), with the self-consistent screening length and with the ballistic one, Eq. (3.28); upper: logarithmic scale, lower: linear scale. The approximation including the self-consistent kinetic screening length (dashed line) fits best the full quantum kinetic solution (solid line).*

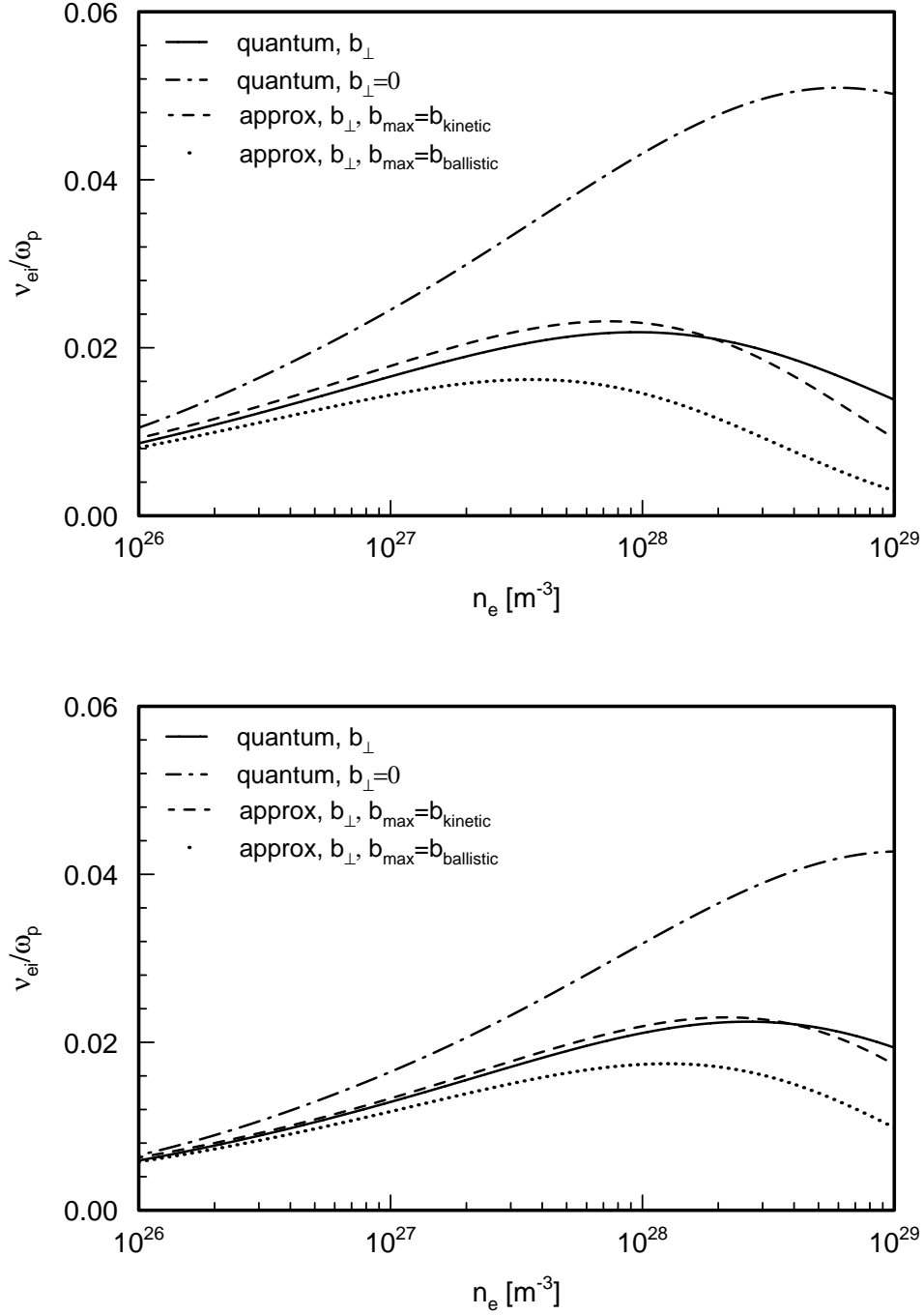


Figure 4.2: *Electron-ion collision frequency as a function of the density ; $Z = 1, T_e = 3 \cdot 10^5$ K = 25.85 eV, $\omega_0/\omega_p = 5$. upper: $\hat{v}_{os}/v_{th} = 1$, lower: $\hat{v}_{os}/v_{th} = 2$. The best approximation to the full quantum kinetic solution (solid line) is the one including the self-consistent kinetic screening length (dashed line). This approximation fails for $\hat{v}_{os}/v_{th} \leq 1$ and $n_e \geq 3 \cdot 10^{28} \text{ m}^{-3}$ (upper figure), because the relations λ_B/λ_D and b_\perp/λ_D are no longer much smaller than one; $\lambda_B/\lambda_D = 0.227$, $b_\perp/\lambda_D = 0.373$ for $n_e = 10^{29} \text{ m}^{-3}$.*

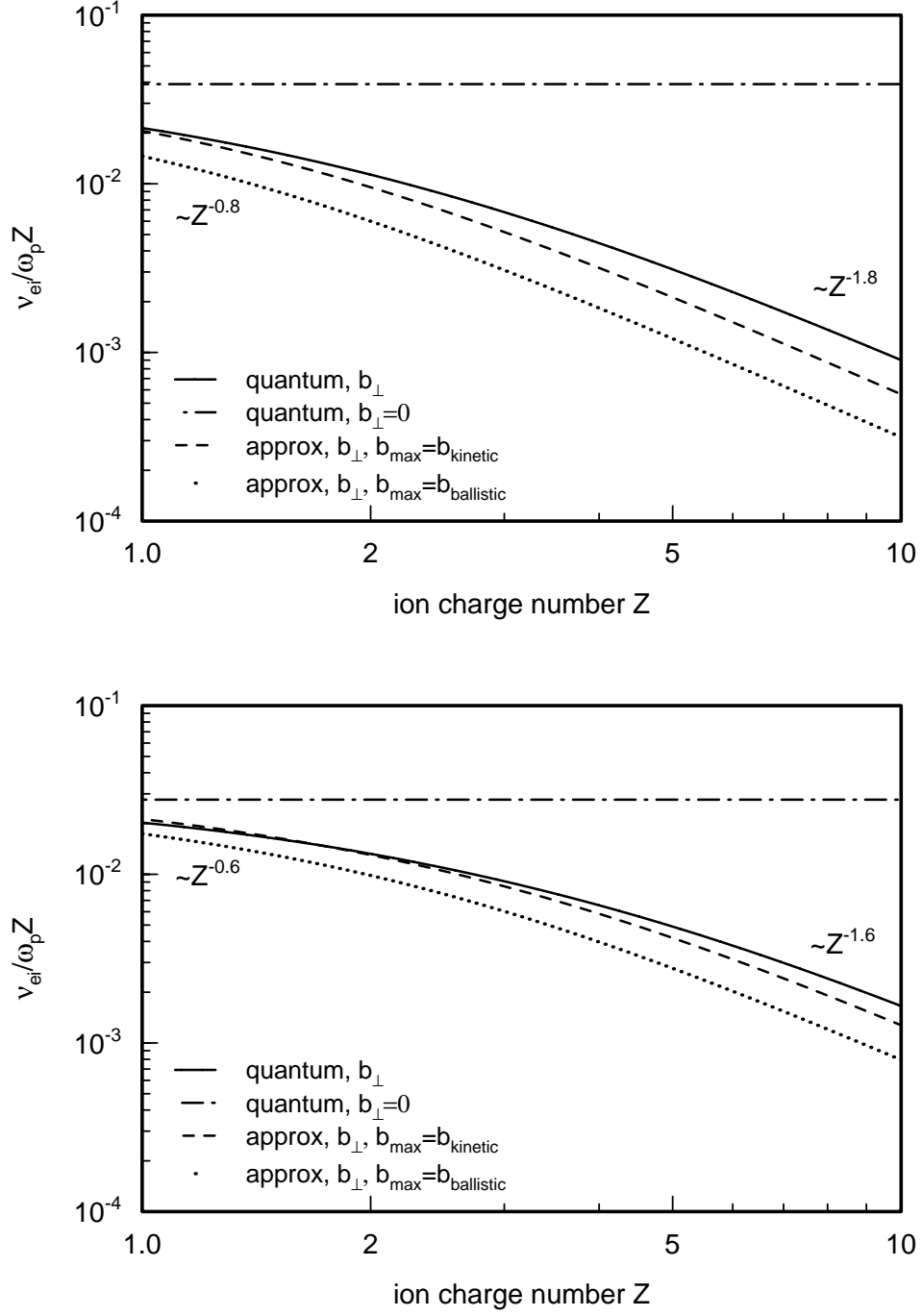


Figure 4.3: *Electron-ion collision frequency normalized by Z as a function of the ion charge number Z ; $n_e = 10^{28} \text{ m}^{-3}$, $T_e = 3 \cdot 10^5 \text{ K} = 25.85 \text{ eV}$, $\omega_0/\omega_p = 5$. upper: $\hat{v}_{os}/v_{th} = 1$, lower: $\hat{v}_{os}/v_{th} = 2$. According to the linear Z dependence of b_{\perp} the relation ν_{ei}/Z is no longer constant.*

We can finish the present investigation with a short and concise summary of the main results:

- The impact of many-particle collisions was discussed. We came to the conclusion that in the mean, due to the velocity and density scaling of the screening length as well as the parameter of rectangular deflection, the influence of *strong* electron-ion *many-body* collisions is small. Most of these are *weak* collisions which can be calculated by first order Born approximation. Nevertheless, the inclusion of *strong binary* collisions is important.
- The quantum kinetic expression for the absorption rate in random phase approximation (RPA) was calculated. It was shown that in general the long-wavelength approximation (LWA) fails. Nevertheless, we could demonstrate that the result for the time averaged absorption rate calculated by using the LWA limit remains valid.
- With the help of the *ballistic model* the kinetic treatment in RPA, which is limited to weak collisions, could be extended analytically for the first time to the case of strong binary collisions. The result is a *combined model* which was, in particular cases, numerically achieved by others adding the static screened T-Matrix to the RPA results.
- The combination of the ballistic and the kinetic treatment led us to *closed analytical* expressions for the absorption rate. It bypasses the difficult summation and integration of a large amount of Bessel functions appearing in the kinetic treatment.
- A so far unknown saturation behavior of the screening length has been found: It becomes constant for large oscillation velocities. The interpretation of this effect in physical terms is in progress.

Appendix A

Explicit Expressions for Propagators

A.1 Free propagators

Due to the missing interaction of the particles the many-body propagator separates into 1-particle propagators:

$$\uparrow_{1\dots N}^\tau = \uparrow_1^\tau \dots \uparrow_N^\tau \quad .$$

The most simple propagator describes the free movement of the particle with momentum \vec{p}_j acting as a shift operator:

$$\begin{aligned} \uparrow_1^\tau f(\vec{r}_1, \vec{p}_1) &= e^{-\tau \frac{\vec{p}_1}{m_1} \frac{\partial}{\partial \vec{r}_1}} f(\vec{r}_1, \vec{p}_1) = f(\vec{r}_1 - \tau \frac{\vec{p}_1}{m_1}, \vec{p}_1) \\ (\uparrow_1^\tau)^{-1} = \downarrow_1^\tau &= e^{+\tau \frac{\vec{p}_1}{m_1} \frac{\partial}{\partial \vec{r}_1}} \\ \uparrow_1^\tau f g &= [\uparrow_1^\tau f] [\uparrow_1^\tau g] \quad . \end{aligned}$$

The expression for the propagator including a time but not position dependent field \vec{F} is given by a shift in position and, after that, a shift in momentum:

$$\begin{aligned} \mathcal{L}_1 &= \mathcal{L}_1^0 + \mathcal{L}^{\text{ex}} &= & -\frac{i}{m_1} \vec{p}_1 \frac{\partial}{\partial \vec{r}_1} - i \vec{F} \frac{\partial}{\partial \vec{p}_1} \\ \uparrow_1^\tau &= e^{-i \int^\tau \mathcal{L}_1} &= & e^{-i \int^\tau \mathcal{L}_1^0 + \mathcal{L}^{\text{ex}}} \\ & & \stackrel{[\text{Eq. (2.10)}]}{=} & e^{-i \int^\tau \mathcal{L}^{\text{ex}}} e^{-i \int^\tau e^{i \int^\tau \mathcal{L}^{\text{ex}}} \mathcal{L}_1^0 e^{-i \int^\tau \mathcal{L}^{\text{ex}}} \\ -e^{i \int^\tau \mathcal{L}^{\text{ex}}} i \mathcal{L}_1^0 e^{-i \int^\tau \mathcal{L}^{\text{ex}}} & &= & -e^{\int^\tau \vec{F} \frac{\partial}{\partial \vec{p}_1}} \frac{\vec{p}_1}{m_1} \frac{\partial}{\partial \vec{r}_1} e^{-\int^\tau \vec{F} \frac{\partial}{\partial \vec{p}_1}} \\ & &= & -\frac{1}{m_1} \left[e^{\int^\tau \vec{F} \frac{\partial}{\partial \vec{p}_1}} \vec{p}_1 \right] \cdot \frac{\partial}{\partial \vec{r}_1} e^{\int^\tau \vec{F} \frac{\partial}{\partial \vec{p}_1}} e^{-\int^\tau \vec{F} \frac{\partial}{\partial \vec{p}_1}} \end{aligned}$$

$$\begin{aligned}
&= -\frac{1}{m_1} \left(\vec{p}_1 + \int^{\tau'} \vec{F} \right) \frac{\partial}{\partial \vec{r}_1} \\
\Rightarrow & \boxed{\begin{aligned} \uparrow_1^\tau &= e^{-\int^{\tau} \vec{F} \frac{\partial}{\partial \vec{p}_1}} e^{-\frac{1}{m_1} (\tau \vec{p}_1 + \int^{\tau} \int^{\tau'} \vec{F}) \frac{\partial}{\partial \vec{r}_1}} \\ \downarrow_1^\tau &= e^{+\frac{1}{m_1} (\tau \vec{p}_1 + \int^{\tau} \int^{\tau'} \vec{F}) \frac{\partial}{\partial \vec{r}_1}} e^{+\int^{\tau} \vec{F} \frac{\partial}{\partial \vec{p}_1}} \end{aligned}} \quad (\text{A.1})
\end{aligned}$$

A.2 Propagators including first order pair interaction

We calculate the first order of the ladder-propagator (2.9). The 1-particle propagators ($\uparrow_{12}^\tau = \uparrow_1^\tau \uparrow_2^\tau$) could contain a time-dependent external field:

$$\begin{aligned}
\left| \begin{array}{c} \text{---} \\ \text{---} \end{array} \right| &= \int_0^{\tau'} \downarrow_{12}^\tau \text{---} \uparrow_{12}^\tau \quad (\text{A.2}) \\
&= \int_0^{\tau'} \downarrow_{12}^\tau \frac{\partial \Phi(1,2)}{\partial \vec{r}_1} \left(\frac{\partial}{\partial \vec{p}_1} - \frac{\partial}{\partial \vec{p}_2} \right) \uparrow_{12}^\tau \\
&= \int_0^{\tau'} \left[\downarrow_{12}^\tau \frac{\partial \Phi(1,2)}{\partial \vec{r}_1} \right] \downarrow_{12}^\tau \left(\frac{\partial}{\partial \vec{p}_1} - \frac{\partial}{\partial \vec{p}_2} \right) \uparrow_{12}^\tau \\
&= \int_0^{\tau'} \left[\frac{\partial}{\partial \vec{r}_1} \downarrow_{12}^\tau \Phi(1,2) \right] \left(\frac{\partial}{\partial \vec{p}_1} - \frac{\tau}{m_1} \frac{\partial}{\partial \vec{r}_1} - \frac{\partial}{\partial \vec{p}_2} + \frac{\tau}{m_2} \frac{\partial}{\partial \vec{r}_2} \right) .
\end{aligned}$$

Thinking on the Coulomb interaction and the external field of the laser in dipole approximation leads us to the potential term Fourier transformed with respect to the particle distance

$$\downarrow_{12}^\tau \Phi(1,2) = \frac{q_1 q_2}{4\pi\epsilon_0} \int \frac{d^3 k}{(2\pi)^3} \frac{1}{k^2} e^{i\vec{k} \left(\vec{r}_1 + \frac{\tau}{m_1} \vec{p}_1 - \vec{r}_2 - \frac{\tau}{m_2} \vec{p}_2 + \left(\frac{q_1}{m_1} - \frac{q_2}{m_2} \right) \int^{\tau} \int^{\tau'} \vec{E} \right)} .$$

If the electric field oscillates periodically like $E(t) = E_0 \cos \omega_0 t$, this term can be transformed into a Bessel sum (J_l Bessel function of order l):

$$\begin{aligned}
\downarrow_{12}^\tau \Phi(1,2) &= \frac{q_1 q_2}{4\pi\epsilon_0} \sum_{l=-\infty}^{l=+\infty} (-i)^l e^{il\omega_0\tau} \\
&\quad \int \frac{d^3 k}{(2\pi)^3} \frac{1}{k^2} J_l \left(\vec{k} \left(\frac{q_1}{m_1} - \frac{q_2}{m_2} \right) \frac{\vec{E}_0}{\omega_0^2} \right) e^{i\vec{k} \left(\vec{r}_1 + \frac{\tau}{m_1} \vec{p}_1 - \vec{r}_2 - \frac{\tau}{m_2} \vec{p}_2 + \left(\frac{q_1}{m_1} - \frac{q_2}{m_2} \right) \frac{\vec{E}_0}{\omega_0^2} \right)} .
\end{aligned}$$

With regard to the RPA approximation we look at the operator (A.2) after the reduction of one particle. Again, we choose the Fourier representation with respect to the particle distance for the potential term:

$$\begin{aligned}
\int_0^{\tau'} \int d1 \downarrow_{12}^{\tau} \sim \uparrow_{12}^{\tau} &= i \int_0^{\tau'} \int \frac{d^3 k}{(2\pi)^3} \vec{k} \Phi_{12}(k) e^{i\vec{k} \left(\left(\frac{q_1}{m_1} - \frac{q_2}{m_2} \right) \int_0^{\tau'} \vec{E} - \vec{r}_2 - \frac{\tau}{m_2} \vec{p}_2 \right)} \\
&\quad \int d^3 r_1 d^3 p_1 e^{i\vec{k}(\vec{r}_1 + \frac{\tau}{m_1} \vec{p}_1)} \left(\frac{\partial}{\partial \vec{p}_1} - \frac{\tau}{m_1} \frac{\partial}{\partial \vec{r}_1} - \frac{\partial}{\partial \vec{p}_2} + \frac{\tau}{m_2} \frac{\partial}{\partial \vec{r}_2} \right) \\
&= i \int_0^{\tau'} \int \frac{d^3 k}{(2\pi)^3} \vec{k} \Phi_{12}(k) e^{i\vec{k} \left(\left(\frac{q_1}{m_1} - \frac{q_2}{m_2} \right) \int_0^{\tau'} \vec{E} - \vec{r}_2 - \frac{\tau}{m_2} \vec{p}_2 \right)} \\
&\quad \left(\frac{\tau}{m_1} i\vec{k} - \frac{\tau}{m_1} i\vec{k} - \frac{\partial}{\partial \vec{p}_2} + \frac{\tau}{m_2} \frac{\partial}{\partial \vec{r}_2} \right) \int d^3 r_1 d^3 p_1 e^{i\vec{k}(\vec{r}_1 + \frac{\tau}{m_1} \vec{p}_1)} \\
&= -i \int_0^{\tau'} \int \frac{d^3 k}{(2\pi)^3} \vec{k} \Phi_{12}(k) e^{i\vec{k} \left(\left(\frac{q_1}{m_1} - \frac{q_2}{m_2} \right) \int_0^{\tau'} \vec{E} - \vec{r}_2 - \frac{\tau}{m_2} \vec{p}_2 \right)} \\
&\quad \left(\frac{\partial}{\partial \vec{p}_2} - \frac{\tau}{m_2} \frac{\partial}{\partial \vec{r}_2} \right) \int d^3 r_1 d^3 p_1 e^{i\vec{k}(\vec{r}_1 + \frac{\tau}{m_1} \vec{p}_1)} \tag{A.3}
\end{aligned}$$

Mainly this operator acts as a Fourier transform.

Appendix B

RPA approximation

At first the calculation for the classical case is done. The extension to the quantum regime will be obvious. We need the expressions which build up when the operator (A.3) acts n times on the product of distribution functions at $t = 0$. Calculating the Fourier action of (A.3) when again acting on itself we get $[\vec{\eta}_{jk}(\tau) = (\frac{q_j}{m_j} - \frac{q_k}{m_k}) \int^\tau \int^{\tau'} \vec{E}]$

$$\begin{aligned}
& -i \int d^3 r_2 d^3 p_2 e^{i\vec{k}'(\vec{r}_2 + \frac{\tau'}{m_2} \vec{p}_2)} \int_0^{\tau'} \int \frac{d^3 k}{(2\pi)^3} \Phi_{12}(k) e^{i\vec{k}(\vec{\eta}_{12}(\tau) - \vec{r}_2 - \frac{\tau}{m_2} \vec{p}_2)} \otimes \\
& \vec{k} \left(\frac{\partial}{\partial \vec{p}_2} - \frac{\tau}{m_2} \frac{\partial}{\partial \vec{r}_2} \right) \int d^3 r_1 d^3 p_1 e^{i\vec{k}(\vec{r}_1 + \frac{\tau}{m_1} \vec{p}_1)} \\
& = -i \int_0^{\tau'} \int \frac{d^3 k}{(2\pi)^3} \Phi_{12}(k) e^{i\vec{k}\vec{\eta}_{12}(\tau)} i\vec{k}\vec{k}' \frac{\tau' - \tau}{m_2} \otimes \\
& \int d^3 r_2 d^3 p_2 e^{i\vec{r}_2(\vec{k}' - \vec{k}) + i\frac{\vec{p}_2}{m_2}(\vec{k}'\tau' - \vec{k}\tau)} \int d^3 r_1 d^3 p_1 e^{i\vec{k}(\vec{r}_1 + \frac{\tau}{m_1} \vec{p}_1)} .
\end{aligned}$$

So, the second order of the RPA approximation is:

$$\begin{aligned}
& \int_0^{\tau''} \int d2 \downarrow_{23}^{\tau'} \sim \uparrow_{23}^{\tau'} \int_0^{\tau'} \int d1 \downarrow_{12}^{\tau} \sim \uparrow_{12}^{\tau} \\
& = (-i) \int_0^{\tau''} \int \frac{d^3 k'}{(2\pi)^3} \Phi_{23}(k') e^{i\vec{k}'\vec{\eta}_{23}(\tau')} e^{-i\vec{k}'(\vec{r}_3 + \frac{\tau'}{m_3} \vec{p}_3)} \vec{k}' \left(\frac{\partial}{\partial \vec{p}_3} - \frac{\tau'}{m_3} \frac{\partial}{\partial \vec{r}_3} \right) \otimes \\
& (-i) \int_0^{\tau'} \int \frac{d^3 k}{(2\pi)^3} \Phi_{12}(k) e^{i\vec{k}\vec{\eta}_{12}(\tau)} i\vec{k}\vec{k}' \frac{\tau' - \tau}{m_2} \otimes
\end{aligned}$$

$$\int d2 \ e^{i\vec{r}_2(\vec{k}'-\vec{k})+i\frac{\vec{p}_2}{m_2}(\vec{k}'\tau'-\vec{k}\tau)} \int d1 \ e^{i\vec{k}(\vec{r}_1+\frac{\tau}{m_1}\vec{p}_1)} .$$

In order to understand the scheme which builds up, we have a look at the third order:

$$\begin{aligned} & \int_0^{\tau'''} \int d3 \ \downarrow_{34}^{\tau''} \sim \uparrow_{34}^{\tau''} \int_0^{\tau''} \int d2 \ \downarrow_{23}^{\tau'} \sim \uparrow_{23}^{\tau'} \int_0^{\tau'} \int d1 \ \downarrow_{12}^{\tau} \sim \uparrow_{12}^{\tau} \\ = & \quad (-i) \int_0^{\tau'''} \int \frac{d^3 k''}{(2\pi)^3} \Phi_{34}(k'') e^{i\vec{k}''\vec{\eta}_{34}(\tau'')} e^{-i\vec{k}''(\vec{r}_4+\frac{\tau''}{m_4}\vec{p}_4)} \vec{k}'' \left(\frac{\partial}{\partial \vec{p}_4} - \frac{\tau''}{m_4} \frac{\partial}{\partial \vec{r}_4} \right) \otimes \\ & \quad (-i) \int_0^{\tau''} \int \frac{d^3 k'}{(2\pi)^3} \Phi_{23}(k') e^{i\vec{k}'\vec{\eta}_{23}(\tau')} i\vec{k}'\vec{k}'' \frac{\tau''-\tau'}{m_3} \otimes \\ & \quad (-i) \int_0^{\tau'} \int \frac{d^3 k}{(2\pi)^3} \Phi_{12}(k) e^{i\vec{k}\vec{\eta}_{12}(\tau)} i\vec{k}\vec{k}' \frac{\tau'-\tau}{m_2} \otimes \\ & \quad \int d3 \ e^{i\vec{r}_3(\vec{k}''-\vec{k}')+i\frac{\vec{p}_3}{m_3}(\vec{k}''\tau''-\vec{k}'\tau')} \int d2 \ e^{i\vec{r}_2(\vec{k}'-\vec{k})+i\frac{\vec{p}_2}{m_2}(\vec{k}'\tau'-\vec{k}\tau)} \int d1 \ e^{i\vec{k}(\vec{r}_1+\frac{\tau}{m_1}\vec{p}_1)} . \end{aligned}$$

Further on we assume that the plasma is homogenous at $t = 0$. So, the distribution functions do not depend on the position at the beginning and the Fourier integrals due to \vec{r}_1, \vec{r}_2 give products of delta functions; and the k -integrations simplifies to:

$$\begin{aligned} & \int_0^{\tau'''} \int d3 \ \downarrow_{34}^{\tau''} \sim \uparrow_{34}^{\tau''} \int_0^{\tau''} \int d2 \ \downarrow_{23}^{\tau'} \sim \uparrow_{23}^{\tau'} \int_0^{\tau'} \int d1 \ \downarrow_{12}^{\tau} \sim \uparrow_{12}^{\tau} \\ = & \quad (-i) \int_0^{\tau'''} \int \frac{d^3 k}{(2\pi)^3} \Phi_{34}(k) e^{i\vec{k}\vec{\eta}_{34}(\tau'')} e^{-i\vec{k}(\vec{r}_4+\frac{\tau''}{m_4}\vec{p}_4)} \vec{k} \frac{\partial}{\partial \vec{p}_4} \otimes \\ & \quad (-i) \int_0^{\tau''} \Phi_{23}(k) e^{i\vec{k}\vec{\eta}_{23}(\tau')} i k^2 \frac{\tau''-\tau'}{m_3} \int d^3 p_3 e^{i\frac{\vec{p}_3}{m_3}\vec{k}(\tau''-\tau')} \otimes \\ & \quad (-i) \int_0^{\tau'} \Phi_{12}(k) e^{i\vec{k}\vec{\eta}_{12}(\tau)} i k^2 \frac{\tau'-\tau}{m_2} \int d^3 p_2 e^{i\frac{\vec{p}_2}{m_2}\vec{k}(\tau'-\tau)} \otimes \\ & \quad \int d^3 p_1 d^3 r_1 e^{i\vec{k}(\vec{r}_1+\frac{\tau}{m_1}\vec{p}_1)} . \end{aligned}$$

For higher orders we will get more and more terms than the two middle ones in the above equation. The particle-species being different depend on the electric field of the laser

by the $\vec{\eta}_{ij}$ terms. For the same particle species these terms vanish. Due to the large ion mass we neglect all contributions of the ions but the first one. That means, particle one is considered to be an ion and the rest to be electrons, $\vec{\eta}_{12} = -\vec{\eta}_{ei}$ and $\Phi_{12}(k) = \Phi_{ei}(k)$. The time integrals are of convolution type. By using the Laplace transform the terms could be factorized. For the n th order operator acting on the product of n homogenous distribution functions f_e and on one inhomogeneous function f_i we get

$$\begin{aligned} \left| \text{---} \text{---} \text{---} \cdots \text{---} \right| &= (-i) \int_0^t \int \frac{d^3 k}{(2\pi)^3} \Phi_{ei}(k) e^{-i\vec{k}(\vec{r}_e + \frac{\tau}{m_e} \vec{p}_e)} \vec{k} \frac{\partial f_e^0(\vec{p}_e)}{\partial \vec{p}_e} \\ &\times \int_{c-i\infty}^{c+i\infty} \frac{ds}{2\pi i} e^{s\tau} (\Pi(\vec{k}, s) \Phi_{ee}(k))^{n-1} \\ &\times \int_0^\infty d\tau' e^{-s\tau'} e^{-i\vec{k}\vec{\eta}_{ei}(\tau')} \int d^3 p_i d^3 r_i e^{i\vec{k}(\vec{r}_i + \frac{\tau'}{m_i} \vec{p}_i)} f_i^0(\vec{r}_i, \vec{p}_i) \end{aligned}$$

with the RPA polarization function

$$\Pi(\vec{k}, s) = -i \int_0^\infty d\tau e^{-s\tau} i k^2 \frac{\tau}{m_e} \int d^3 p_e e^{i\frac{\vec{p}_e}{m_e} \vec{k} \tau} f_e^0(\vec{p}_e) .$$

Summing up all orders starting at $n = 1$ the terms $(\Pi\Phi)^{n-1}$ result in a geometric sum. Adding the free propagator Eq. (2.11) we get the one particle electron distribution function in RPA approximation:

$$\begin{aligned} f_e(\vec{r}_e, \vec{p}_e, t) &= \uparrow_e^t f_e^0(\vec{p}_e) - \uparrow_e^t \int_0^t \frac{d^3 k}{(2\pi)^3} \Phi_{ei}(k) e^{-i\vec{k}(\vec{r}_e + \frac{\tau}{m_e} \vec{p}_e)} \vec{k} \frac{\partial f_e^0(\vec{p}_e)}{\partial \vec{p}_e} \\ &\times \int_{c-i\infty}^{c+i\infty} \frac{ds}{2\pi} e^{s\tau} \frac{1}{1 - \Pi(\vec{k}, s) \Phi_{ee}(k)} \\ &\times \int_0^\infty d\tau' e^{-s\tau'} e^{-i\vec{k}\vec{\eta}_{ei}(\tau')} \int d^3 p_i d^3 r_i e^{i\vec{k}(\vec{r}_i + \frac{\tau'}{m_i} \vec{p}_i)} f_i^0(\vec{r}_i, \vec{p}_i) \end{aligned} \quad (\text{B.1})$$

The calculations done before are very similar in the quantum case, as all actions done on the classical derivative $\vec{k} \left(\frac{\partial}{\partial \vec{p}} - \frac{\tau}{m} \frac{\partial}{\partial \vec{r}} \right)$ also perform on the quantum one - $\sinh \left[\frac{\hbar \vec{k}}{2} \left(\frac{\partial}{\partial \vec{p}} - \frac{\tau}{m} \frac{\partial}{\partial \vec{r}} \right) \right]$:

$$\begin{aligned} f_e^{\text{qu}}(\vec{r}_e, \vec{p}_e, t) &= \uparrow_e^t f_e^0(\vec{p}_e) - \uparrow_e^t \frac{2}{\hbar} \int_0^t \frac{d^3 k}{(2\pi)^3} \Phi_{ei}(k) e^{-i\vec{k}(\vec{r}_e + \frac{\tau}{m_e} \vec{p}_e)} \sinh \left[\frac{\hbar \vec{k}}{2} \frac{\partial}{\partial \vec{p}_e} \right] f_e^0(\vec{p}_e) \\ &\times \int_{c-i\infty}^{c+i\infty} \frac{ds}{2\pi} e^{s\tau} \frac{1}{1 - \Pi^{\text{qu}}(\vec{k}, s) \Phi_{ee}(k)} \\ &\times \int_0^\infty d\tau' e^{-s\tau'} e^{-i\vec{k}\vec{\eta}_{ei}(\tau')} \int d^3 p_i d^3 r_i e^{i\vec{k}(\vec{r}_i + \frac{\tau'}{m_i} \vec{p}_i)} f_i^0(\vec{r}_i, \vec{p}_i) \end{aligned} \quad (\text{B.2})$$

where

$$\Pi^{\text{qu}}(\vec{k}, s) = -\frac{2i}{\hbar} \int_0^\infty d\tau e^{-s\tau} \sinh \left(\frac{i\hbar}{2} k^2 \frac{\tau}{m_e} \right) \int d^3 p_e e^{i\frac{\vec{p}_e}{m_e} \vec{k} \tau} f_e^0(\vec{p}_e)$$

denotes the quantum kinetic polarization function.

We can immediately extract the effective potential acting on the electrons:

$$\begin{aligned} \Phi_{\text{eff}}(\vec{r}_e, t) &= \int_{c-i\infty}^{c+i\infty} \frac{ds}{2\pi} e^{st} \int \frac{d^3k}{(2\pi)^3} e^{i\vec{k}\vec{r}_e} \frac{\Phi_{ei}(k)}{1 - \Pi(\vec{k}, s)\Phi_{ee}(k)} \\ &\times \int_0^\infty d\tau' e^{-s\tau'} e^{-i\vec{k}\vec{\eta}_{ei}(\tau')} \int d^3p_i d^3r_i e^{i\vec{k}(\vec{r}_i + \frac{\tau'}{m_i}\vec{p}_i)} f_i^0(\vec{r}_i, \vec{p}_i) \end{aligned} \quad (\text{B.3})$$

Further on, the equilibrium distribution functions are assumed to be Maxwellian,

$$f_{e,i}^0 = \frac{n_{e,i}^0}{(2\pi m_{e,i}^2 v_{e,i}^2)^{3/2}} e^{-\frac{p_{e,i}^2}{2v_{e,i}^2 m_{e,i}^2}}.$$

Additionally, we take a delta function for the space dependence of the initial ion distribution function, $\delta(\vec{r}_i - \vec{r}_0)$. With the thermal electron/ion velocity $v_{e,i}$ and the De Broglie wave number $k_B = (\hbar/2m_e v_e)^{-1}$ the classical and quantum kinetic expressions for the polarization Π , the dielectric function ϵ as well as the electron distribution function result in

$$\begin{aligned} f_e(\vec{r}_e, \vec{p}_e, t) &= \uparrow_e^t f_e^0(p_e) - \uparrow_e^t \frac{n_e^0}{(2\pi)^3 v_e^5 m_e^5} \int_0^t \int \frac{d^3k}{(2\pi)^3} \Phi_{\text{eff}}(\vec{k}, \tau) \\ &\times e^{-i\vec{k}(\vec{r}_e + \frac{\tau}{m_e}\vec{p}_e)} e^{-\frac{p_e^2}{2v_e^2 m_e^2}} \vec{k}\vec{p}_e \end{aligned} \quad (\text{B.4})$$

$$\begin{aligned} f_e^{\text{qu}}(\vec{r}_e, \vec{p}_e, t) &= \uparrow_e^t f_e^0(p_e) - \uparrow_e^t \frac{2n_e^0}{\hbar(2\pi)^3 v_e^3 m_e^3} \int_0^t \int \frac{d^3k}{(2\pi)^3} \Phi_{\text{eff}}^{\text{qu}}(\vec{k}, \tau) \\ &\times e^{-i\vec{k}(\vec{r}_e + \frac{\tau}{m_e}\vec{p}_e)} e^{-\frac{p_e^2}{2v_e^2 m_e^2} - \frac{k^2}{2k_B^2}} \sinh\left(\frac{\vec{k}\vec{p}_e}{k_B v_e m_e}\right) \end{aligned} \quad (\text{B.5})$$

$$\epsilon(k, s) = 1 - \Pi(k, s)\Phi_{ee}(k) \quad (\text{B.6})$$

$$\Pi(k, s) = \frac{n_e^0}{m_e v_e^2} \left(1 - \sqrt{\frac{\pi}{2}} \frac{s}{k v_e} e^{\frac{1}{2}\left(\frac{s}{k v_e}\right)^2} \text{erfc}\left(\frac{s}{\sqrt{2}k v_e}\right) \right) \quad (\text{B.7})$$

$$\begin{aligned} \Pi^{\text{qu}}(k, s) &= \frac{i}{\hbar} \frac{n_e^0}{k v_e} \sqrt{\frac{\pi}{2}} \left[e^{\frac{1}{2}\left(\frac{s}{k v_e} + \frac{ik}{k_B}\right)^2} \text{erfc}\left(\frac{s}{\sqrt{2}k v_e} + \frac{ik}{\sqrt{2}k_B}\right) - \right. \\ &\left. e^{\frac{1}{2}\left(\frac{s}{k v_e} - \frac{ik}{k_B}\right)^2} \text{erfc}\left(\frac{s}{\sqrt{2}k v_e} - \frac{ik}{\sqrt{2}k_B}\right) \right]. \end{aligned} \quad (\text{B.8})$$

$$\Phi_{\text{eff}}(\vec{k}, \tau) = \int_{c-i\infty}^{c+i\infty} \frac{ds}{2\pi} e^{s\tau} e^{i\vec{k}\vec{r}_0} \frac{\Phi_{ei}(k)}{\epsilon(k, s)} \int_0^\infty d\tau' e^{-s\tau'} e^{-i\vec{k}\vec{\eta}_{ei}(\tau')} e^{-(k\tau v_i)^2} \quad (\text{B.9})$$

$$\vec{\eta}_{ei}(\tau) = \left(\frac{e}{m_e} - \frac{Ze}{m_i} \right) \int^\tau \int^{\tau'} \vec{E}(\tau')$$

Appendix C

Wigner Representation of the Kinetic Hierarchy

The content of this chapter is mostly taken unchanged from the book of Michael Bonitz [23] and should help the reader who is not quite familiar with the Wigner representation of the BBGKY-hierarchy. The only change was the substitution of \bar{p} by η to remain consistent to the notation of the current work.

We consider the BBGKY-hierarchy in coordinate representation, which involves matrices of the type $F_{1\dots s}(r'_1, \dots, r'_s; r''_1, \dots, r''_s, t)$:

$$\begin{aligned} & \left\{ i\hbar \frac{\partial}{\partial t} - H_{1\dots k}(r_1, \dots, r_k) + H_{1\dots k}(r'_1, \dots, r'_k) \right\} F_{1\dots k}(r_1, \dots, r_k; r'_1, \dots, r'_k, t) \\ &= n \sum_{i=1}^k \sum_{s_{k+1}} \int d\mathbf{r}_{k+1} \{ V(\mathbf{r}_i - \mathbf{r}_{k+1}) - V(\mathbf{r}'_i - \mathbf{r}_{k+1}) \} \\ & \quad \times F_{k+1}(r_1, \dots, r_{k+1}; r'_1, \dots, r'_k, r_{k+1}, t) . \end{aligned}$$

Introducing center of mass and relative coordinates, R_i and r_i for each particle, according to $r'_i = R_i + r_i/2$ and $r''_i = R_i - r_i/2$, or, vice versa, $R_i = (r'_i + r''_i)/2$ and $r_i = r'_i - r''_i$, the above matrix transforms into

$$\begin{aligned} F_{1\dots s}(r'_1, \dots, r'_s; r''_1, \dots, r''_s, t) &= F_{1\dots s}(R_1 + \frac{r_1}{2}, \dots, R_s + \frac{r_s}{2}; R_1 - \frac{r_1}{2}, \dots, R_s - \frac{r_s}{2}, t) \\ &= \tilde{F}_{1\dots s}(R_1, r_1, \dots, R_s, r_s, t) = \frac{1}{n^s} \tilde{f}_{1\dots s}(R_1, r_1, \dots, R_s, r_s, t) . \end{aligned}$$

We can rewrite the hierarchy equations suppressing the spin variables:

$$\begin{aligned} & \left\{ i\hbar \frac{\partial}{\partial t} - H_{1\dots k}(R_1 + \frac{r_1}{2}, \dots, R_k + \frac{r_k}{2}) + H_{1\dots k}(R_1 - \frac{r_1}{2}, \dots, R_k - \frac{r_k}{2}) \right\} \tilde{f}_{1\dots k}(R_1, r_1, \dots, R_k, r_k, t) \\ &= \sum_{i=1}^k \int dR_{k+1} \left\{ V(R_i - R_{k+1} + \frac{r_i}{2}) - V(R_i - R_{k+1} - \frac{r_i}{2}) \right\} \tilde{f}_{k+1}(R_1, r_1, \dots, R_{k+1}, 0, t) . \quad (\text{C.1}) \end{aligned}$$

The kinetic energy terms and the binary interaction potentials V_{ij} in the Hamiltonians transform to ($r_{ij} = r_i - r_j$; $R_{ij} = R_i - R_j$)

$$\begin{aligned} V(r'_i - r'_j) - V(r''_i - r''_j) &= V(R_{ij} + \frac{r_{ij}}{2}) - V(R_{ij} - \frac{r_{ij}}{2}) \\ -\frac{\hbar^2}{2m_i} (\nabla_{r'_i}^2 - \nabla_{r''_i}^2) &= -2 \frac{\hbar^2}{2m_i} \nabla_{R_i} \nabla_{r_i}. \end{aligned}$$

We now introduce the Wigner transformation with respect to the relative coordinates r_1, \dots, r_s and the inverse transform according to

$$\begin{aligned} f_{1\dots s}(R_1, p_1, \dots, R_s, p_s, t) &= \int \frac{dr_1}{(2\pi\hbar)^3} \cdots \frac{dr_s}{(2\pi\hbar)^3} \exp\{-i(p_1 r_1 + \cdots + p_s r_s)/\hbar\} \\ &\quad \times \tilde{f}_{1\dots s}(R_1, r_1, \dots, R_s, r_s, t) \quad (C.2) \end{aligned}$$

$$\begin{aligned} \tilde{f}_{1\dots s}(R_1, r_1, \dots, R_s, r_s, t) &= \int dp_1 \dots dp_s \exp\{i(p_1 r_1 + \cdots + p_s r_s)/\hbar\} \\ &\quad \times f_{1\dots s}(R_1, p_1, \dots, R_s, p_s, t). \quad (C.3) \end{aligned}$$

The Wigner transform (C.2) of Eq. (C.1) is

$$\left\{ i\hbar \frac{\partial}{\partial t} + i\hbar \sum_{i=1}^k \frac{p_i}{m_i} \nabla_{R_i} \right\} f(R_i, p_i, \dots, R_k, p_k, t) - \sum_{1 \leq i < j \leq k} V_k^{(ij)} - \sum_i U_k^{(i)} = \sum_{i=1}^k F_{k+1}^{(i)},$$

where only the non-trivial terms are those containing the external potential or the interaction potential which are denoted $U_k^{(i)}$, $V_k^{(ij)}$ and $F_{k+1}^{(i)}$, respectively. We consider $V_k^{(ij)}$ more in detail,

$$\begin{aligned} V_k^{(ij)} &= \int \frac{dr_1}{(2\pi\hbar)^3} \cdots \frac{dr_k}{(2\pi\hbar)^3} \exp\left\{-\frac{i}{\hbar}(p_1 r_1 + \cdots + p_k r_k)\right\} \\ &\quad \times \left\{ V(R_{ij} + \frac{r_{ij}}{2}) - V(R_{ij} - \frac{r_{ij}}{2}) \right\} \tilde{f}_{1\dots k}(R_1, r_1, \dots, R_k, r_k, t) \end{aligned}$$

which, after using for \tilde{f} Eq. (C.3), transforms to

$$\begin{aligned} &\int \frac{dr_1}{(2\pi\hbar)^3} \cdots \frac{dr_k}{(2\pi\hbar)^3} d\eta_1 \dots d\eta_k \exp\left\{-\frac{i}{\hbar}(p_1 r_1 + \cdots + p_k r_k - \eta_1 r_1 - \eta_k r_k)\right\} \\ &\quad \times \left\{ V(R_{ij} + \frac{r_{ij}}{2}) - V(R_{ij} - \frac{r_{ij}}{2}) \right\} f_{1\dots k}(R_1, \eta_1, \dots, R_k, \eta_k, t). \end{aligned}$$

The integrals over all coordinates and momenta, except those with the indices i and j can be carried out according to

$$\int \frac{dr_a}{(2\pi\hbar)^3} d\eta_a \exp\{-i(p_a - \eta_a) r_a / \hbar\} G(\eta_a) = G(p_a),$$

whereas the argument of the remaining exponential is conveniently rearranged as $p_i r_i + p_j r_j - \eta_i r_i - \eta_j r_j = (p_i - \eta_i)(r_i - r_j) + (p_i - \eta_i + p_j - \eta_j)r_j$. The second term yields $\delta(p_i - \eta_i + p_j - \eta_j)$, and we finally obtain

$$\begin{aligned} V_k^{(ij)} &= \int \frac{dr_{ij}}{(2\pi\hbar)^3} d\eta_i \exp\{-i(p_i - \eta_i) r_{ij} / \hbar\} \\ &\times \left\{ V(R_{ij} + \frac{r_{ij}}{2}) - V(R_{ij} - \frac{r_{ij}}{2}) \right\} \\ &\times f_{1\dots k}(R_1, p_1, \dots, R_i, \eta_i, \dots, R_j, p_i - \eta_i + p_j, \dots, R_k, p_k, t). \end{aligned}$$

In a similar way, we transform $U_k^{(i)}$ and $F_{k+1}^{(i)}$, with the final result

$$\begin{aligned} U_k^{(i)} &= \int \frac{dr_i}{(2\pi\hbar)^3} d\eta_i \exp\{-i(p_i - \eta_i) r_i / \hbar\} \\ &\times \left\{ U(R_i + \frac{r_i}{2}) - U(R_i - \frac{r_i}{2}) \right\} \\ &\times f_{1\dots k}(R_1, p_1, \dots, R_{i-1}, p_{i-1}, R_i, \eta_i, R_{i+1}, p_{i+1}, \dots, R_k, p_k, t), \\ F_{k+1}^{(i)} &= \int \frac{dr_i}{(2\pi\hbar)^3} d\eta_i dR_{k+1} dp_{k+1} \exp\{-i(p_i - \eta_i) r_i / \hbar\} \\ &\times \left\{ V(R_{i,k+1} + \frac{r_i}{2}) - V(R_{i,k+1} - \frac{r_i}{2}) \right\} \\ &\times f_{1\dots k+1}(R_1, p_1, \dots, R_i, \eta_i, \dots, R_k, p_k, R_{k+1}, p_{k+1}, t). \end{aligned}$$

Bibliography

- [1] L. Spitzer, R. Härm, Phys. Rev. **89**, 977 (1953)
- [2] S.I. Braginskii, Rev. Plasma Phys. **1**, 215 (1965)
- [3] J. Dawson, C. Oberman, Phys. Fluids **5** 1514 (1962)
- [4] V. I. Perel', M. Eliashberg, Sov. Phys. JETP **14**, 633 (1962)
- [5] P. Silin, Sov. Phys. JETP **20**, 1510 (1965)
- [6] C.D. Decker, W.B. Mori, J.M. Dawson, T. Katsouleas, Phys. Plasmas **1**, 4043 (1994)
- [7] S. Rand, Phys. Rev. **136**, 231 (1964)
- [8] L. Schlessinger, J. Wright, Phys. Rev. A **20**, 1934 (1979)
- [9] V.P. Silin, S.A. Uryupin, Sov. Phys. JETP **54** 485 (1981)
- [10] H.-J. Kull, L. Plagne, Phys. Plasmas **8**, 5244 (2001)
- [11] G. Hazak, N. Metzler, M. Klapisch, J. Gardner, Phys. Plasmas **9**, 345 (2002)
- [12] D. Kremp, Th. Bornath, M. Bonitz, M. Schlanges, Phys. Rev. E **60**, 4725 (1999)
- [13] Th. Bornath, M. Schlanges, P. Hilse, D. Kremp, Phys. Rev. E **64**, 026414 (2001)
- [14] A. Saemann, Diploma work, *Stossabsorption in starken Laserfeldern*, Darmstadt University of Technology, November 1994
- [15] P. Mulser, A. Saemann, Contr. Plasma Phys. **37**, 211 (1997)
- [16] P. Mulser, F. Cornolti, E. Besuelle, R. Schneider, Phys. Rev. E **63** 016406 (2000)
- [17] R. Schneider, Contr. Plasma Phys. **41** 315 (2001)
- [18] S. Pfalzner, P. Gibbon, Phys. Rev. E **57**, 4698 (1998)
- [19] D.O. Gericke, M. Schlanges, Phys. Rev. E **60** 904 (1999)
- [20] M. Abramowitz, I.A. Stegun, *Handbook of Mathematical Functions*, Dover Publications, 1965, p. 230 (5.1.4.2)

- [21] M. Abramowitz, I.A. Stegun , *Handbook of Mathematical Functions*, Dover Publications, 1965, p. 229 (5.1.11)
- [22] M. Abramowitz, I.A. Stegun , *Handbook of Mathematical Functions*, Dover Publications, 1965, p. 229 (5.1.20)
- [23] M. Bonitz, *Quantum Kinetic Theory*, Teubner Verlag Stuttgart, 1998
- [24] R. Balescu, *Statistical Mechanics of Charged Particles*, John Wiley & Sons 1963
- [25] Yu.L. Klimontovich, *Kinetic Theory of Nonideal Gases and Nonideal Plasmas*, (Nauka, Moscow 1975) (russ.), Engl. transl.:Pergamon Press, Oxford 1982
- [26] D. Zubarev, V. Morozov, G. Röpke, *Statistical Mechanics of Nonequilibrium Processes*, Volume 1 and 2, Akademie Verlag, 1996

Ich versichere hiermit, daß die vorliegende Arbeit selbstständig und ausschließlich unter Zuhilfenahme der angegebenen Hilfsmittel angefertigt wurde.

Desweiteren versichere ich, daß dies meine erste Promotionsarbeit ist.

Lebenslauf

Name:	Ralf Schneider
Geburtstag, -ort:	23.11.1967, Darmstadt
Familienstand:	verheiratet
Schulbildung:	
1974–1978	Elly-Heuss-Knapp Schule in Darmstadt
1978–1987	Georg-Büchner-Schule in Darmstadt
1987	Abitur
1987–1989	Zivildienst
Berufsausbildung:	
01.04.1989–Jan. 1995	Physikstudium an der TU Darmstadt
01.09.1992–Apr. 1995	Hauptpraktikum und Diplomarbeit bei Prof. Mulser (Theoretische Quantenelektronik)
Juni 1995–Juni 2000	Stelle eines wissenschaftlichen Mitarbeiters bei Prof. Mulser (Theoretische Quantenelektronik)
seit 1994	Selbstständige Tätigkeit in der EDV Branche